

Deep discriminant analysis for task-dependent compact network search

Qing Tian, Tal Arbel, James J. Clark
 Centre for Intelligent Machines & ECE Department
 McGill University, Montreal, QC, Canada

qing.tian@mail.mcgill.ca, arbel@cim.mcgill.ca, clark@cim.mcgill.ca

Abstract

Most of today's popular deep architectures are hand-engineered for general purpose applications. However, this design procedure usually leads to massive redundant, useless, or even harmful features for specific tasks. Such unnecessarily high complexities render deep nets impractical for many real-world applications, especially those without powerful GPU support. In this paper, we attempt to derive task-dependent compact models from a deep discriminant analysis perspective. We propose an iterative and proactive approach for classification tasks which alternates between (1) a pushing step, with an objective to simultaneously maximize class separation, penalize co-variances, and push deep discriminants into alignment with a compact set of neurons, and (2) a pruning step, which discards less useful or even interfering neurons. Deconvolution is adopted to reverse 'unimportant' filters' effects and recover useful contributing sources. A simple network growing strategy based on the basic Inception module is proposed for challenging tasks requiring larger capacity than what the base net can offer. Experiments on the MNIST, CIFAR10, and ImageNet datasets demonstrate our approach's efficacy. On ImageNet, by pushing and pruning our grown Inception-88 model, we achieve better-performing models than smaller deep Inception nets grown, residual nets, and famous compact nets at similar sizes. We also show that our grown deep Inception nets (without hard-coded dimension alignment) can beat residual nets of similar complexities.

1. Introduction

Recent years have witnessed a new AI boom powered by deep learning. Due to deep learning, people no longer need to handcraft features, but architectures still require handcrafted tuning, which influences both the quality and quantity of features to be learned. Features are task dependent, we argue so should be network architectures. After all, net architecture is critical in transforming data from a raw complicated space to one where task-specific analysis is easy.

First, architecture complexity determines how much flexibility and freedom we can have in transforming/folding the data space, which influences the task difficulty that can be dealt with. That said, complexity increase can lead to better performance only if its direction is well aligned with task demands. Random or heuristically designed architectures may possibly project data into spaces where data analysis is suboptimal or hard (e.g. too few useful or too many interfering dimensions). In addition, when designing architectures, consideration should be given to the amount and quality of available training data in the task. Otherwise, over-fitting or under-fitting is likely to occur.

Numerous pruning approaches have been proposed to control model complexity. However, many of them focus on the complexity itself while pay no enough attention to whether the complexity increase/decrease follows a task-optimal direction. For example, weights-based solutions assign importance to each weight or a sum of weights with an i.i.d. assumption. However, in convolutional or dense nets, it is patterns, or relations of weights, that cause certain filters to fire. Moreover, many pruning methods are ex post facto, i.e. useful and useless components are already mixed and it is hard to trim one without influencing the other. Therefore, the performance are heavily dependent on the pre-trained model. Aside from pruning, a compact structure design practice is to utilize a random set of 1×1 filters, usually at the module ends (e.g. Inception nets and ResNets). k 1×1 filters reduce feature map dimension to size k . Nevertheless, the utility at that level may reside in a higher or lower dimension space, which respectively lead to irrecoverable information loss or redundancy/overfitting/interference.

In this paper, we propose to derive task-suitable task-dependent compact networks through deep discriminant analysis in the feature space. Instead of counting on an optimally pre-trained model, the proposed approach follows a two-step procedure in iterations. (1) through learning, it proactively unravels useful twisted threads of deep variation and pushes them into alignment with a compact substructure that can be easily decoupled from the rest. (2) With

the essence being held separated from the dregs, the second pruning step simply throws away the inactive, useless, or even harmful dregs over the layers. Cross-layer dependency is tracked by deconvolution based utility reconstruction. We push and prune in a progressive and gradual manner since it helps improve and expedite the convergence at each iteration. We will show, through solving a generalized eigenvalue problem, that the first step can be achieved by simultaneously including deep LDA and covariance penalty terms to the optimization objective. The LDA and covariance terms are calculated per batch at the easily disentangled end (final latent space), but exert influence over the layers. For scenarios where the desired capacity is larger than what the base structure can offer, a simple network growing/expansion strategy is proposed.

In contrast to fixed network architectures, our grow-push-prune pipeline provides an approach capable of generating a range of task-optimal models for different needs and constraints. According to our experiments on the MNIST, CIFAR10, and ImageNet datasets, efficient compact models with comparable or even better accuracies to the base can be derived in our pursuit of task-suitable architectures. In the ImageNet case, our series of grown deep Inception nets beat residual structures at similar complexities without any hard-coded dimension alignment. One of our grown deep Inception network, Inception-88 net, achieves 75.01% accuracy after training with the conventional cross-entropy and L_2 losses. Deep LDA pushing not only pushes utility into alignment with a compact set of latent neuron dimensions but also increases this accuracy to 75.2%. The pruning step leads to a series of compact models with accuracies even higher than our grown deep Inception nets. At a pruning rate of approximately 6%, a pruned model achieves accuracy of 75.36%, better than both unpruned versions. It is worth mentioning that ResNet-50 achieves accuracy of 74.96% at a slightly larger complexity than the grown Inception-88 net in our experiment.

2. Related Work

Neural Networks Pruning and Compression Early approaches date back to the late 1980s. Some pioneering examples include magnitude-based biased weight decay [47], Hessian based Optimal Brain Damage [35] and Optimal Brain Surgeon [17]. Since those approaches were aimed at shallow nets, assumptions that were made, such as a diagonal Hessian in [35], are not necessarily valid for deep neural networks. Reed [52] offers a review for early researches in this area. In the deep learning era, with progressively increasing depths of architectures comes more model complexity. This re-ignited research into network pruning. Han *et al.* [16] abandon weights of small magnitudes by setting them to zero. With compression techniques in [15], this sparsity is desirable for storage and transferring pur-

poses. Other approaches that sparsify networks by setting zeros include [54, 38, 32, 13, 27, 57]. For most of them, the produced sparsity cannot result in direct parameter and computation savings on general machines.

More recently, filter/neuron/channel pruning has gained popularity (e.g. [46, 1, 36, 60, 24, 61, 67, 41, 23]). Instead of setting zeros in weights matrices, they remove rows, columns, depths in weight/convolution matrices. Thus, the resulting architectures are more hardware friendly. They require not only less storage space and transportation bandwidth, but also less computation. Moreover, with fewer intermediate feature maps produced and consumed, the number of slow and energy-consuming memory accesses is also decreased. Although promising pruning rates have been achieved, most pruning works possess one of the following drawbacks: (1) utilities are usually computed locally and not directly related to final classification. Human expert knowledge, such as equating ‘importance’ to magnitude and variance of weights and activation, is usually hard-coded as the importance measure to guide the pruning process. (2) they usually rely on a pre-trained or passively learned model that may not be amenable to pruning. It may be too late to prune after the fact that useful and harmful components are already intertwined together. (3) although some approaches, such as [67, 41], prune on the filter level, they actually rely on an implicit weight-level i.i.d assumption. Neuron importance is defined as the sum of weight importances within a filter.

Aside from pruning, other approaches to reduce model complexity include: (1) bitwidth reduction and quantization [49, 15, 56, 14, 12, 6], (2) filter decomposition [7, 31, 65], (3) knowledge distillation [25], (4) adopting dimension-reducing 1×1 filters [29, 20], (5) utilizing depth-wise separable convolution instead of the regular one [5, 26]. All such techniques can be orthogonal to our method and helpful in further compressing our derived models. That said, they are outside the scope of this paper.

Efficient Deep Architecture Design and Search With the so-called ‘Moore’s law’ coming to an end, efficient yet accurate architectures become more and more favorable. As mentioned above, most modern deep nets utilize compact modules to control complexity, such as SqueezeNet [29], MobileNet [26], ResNets [20] and Inception Nets [58]. A random number of 1×1 filters are usually adopted to reduce dimensionality at either or both ends of such modules. However, an inappropriate number of such filters can cut the information flow through the layer or result in interference and overfitting. AutoML or Neural Architecture Search (NAS) approaches are promising. Most of them fall into one of the two categories: reinforcement learning (policy gradient) based [2, 68, 69, 66] and evolutionary or genetic algorithms based [55, 63, 40, 51, 50]. Since searching

in a theoretically infinite space is impractical, constraints are usually applied to the search space. That being said, each sampled architecture will still need to be trained separately. Given the large number of possible architecture samples, the procedure will be very computationally expensive. For example, the search processes in Zoph *et al.* [68] and Real *et al.* [51, 50] took the authors 28 days on 800 GPUs and one week on 450 GPUs, respectively. Most such works are done on the small CIFAR10 dataset. When it comes to larger datasets, resulting structures from small datasets are usually duplicated or stacked up. Rather than design the entire network, some start with a macro architecture and fill in different substructure samples into each cell (micro search). In ENAS [44], common structures share the same weights and there is no need to train all sampled architectures separately. However, this is a strong assumption without any theoretical justification. In PNAS [37], instead of fully training all the sampled structures, ‘predictors’ are utilized to ‘predict’ the accuracy based on the differences between the new sample and previous ones (e.g. parents in PNAS). In contrast to bottom-up search into infinity, architectures can also be hunted in a top-down manner, starting from a capacity that is big enough for the task difficulty or can be supported by available data and computing resources. Architectures beyond the capacity are likely to result in over-fitting or cannot meet computation/efficiency requirements. Some promising works following this path include [10, 60, 22]. In [10], Frankle and Carbin hypothesize that a large neural network (a bag of lottery tickets) contains a smaller subnetwork (a winning ticket) which, if trained from the start separately, can achieve a similar accuracy to the large structure. The top-down manner of search is important for locating the winning ticket. In [22], He *et al.* propose AutoML also in a top-down fashion to search compact models. They trained a reinforcement learning agent to predict layerwise channel shrinking actions. To gain efficiency, the reward is roughly estimated based on the model accuracy prior to finetuning. Other AutoML approaches include Monte Carlo tree search [43] and accelerated architecture search with weights prediction [4]. Many tricks are usually needed for AutoML algorithms to achieve satisfactory results, such as CutOut, path augmentation, and drop path.

3. Deep LDA dimension reduction in the deep feature space

Most architecture search approaches involve some trial-and-error process. Usually, tens of thousands of sample architectures are evaluated separately or based on some human-injected relationship. It is not much to our surprise that the best one among them achieves a high accuracy. The hyperparameters are usually highly tuned to one particular dataset, possibly reducing its transferrability to others. In

addition, bottom-up search in infinite spaces, such as many evolutionary algorithms, could possibly miss an ‘optimal’ structure in the early stage and never come back to it. Relatively speaking, top-down compact architecture search is less researched. Many existing works in this direction follow a passive pruning idea (e.g., [10]). In this paper, we propose a proactive deep discriminant analysis based approach that tracks down task-desirable compact architectures by exploring a bounded deep feature space. The capacity up-bound can be set according to task difficulty, available data, or computing resources. Our approach iterates between two steps: (1) maximizing and pushing class separation utility to easily pruned substructures (e.g., neurons) and (2) pruning away less useful substructures. These two steps are illustrated in Algorithm 1, and the details about them will be introduced in Sec. 3.1 and 3.2, respectively.

Algorithm 1: Proactive deep discriminant analysis based pushing and pruning

Input: base net architecture (a popular net or grown using our strategy in Sec. 4.2), acceptable accuracy t_{acc}

Output: task-optimal compact models

while $accuracy \geq t_{acc}$ **do**

Step 1 \rightarrow **Pushing**

 training the net with the deep LDA pushing objectives added (red components in Fig. 1)

Step 2 \rightarrow **Pruning**

 pruning less useful components based on deconv source recovery

end

3.1. Pushing step

The room for complexity reduction in a deep net mainly comes from the less useful and redundant structures. Unlike after-the-fact pruning approaches, we explicitly embed these considerations into the loss function. We leverage LDA to boost class separation and utilize covariance losses to penalize redundancies. As we will show later, these terms simultaneously maximize and unravel useful information flow transferred over the network and push discriminant power into a small set of decision-making neurons. The pushing step is demonstrated as Figure 1. The deep LDA and covariance penalty terms are computed at the last latent space (after ReLU) because: (1) it is directly related to decision making and accepts information from all other layers, (2) the linear assumption of LDA is reasonable or at least easily enforced, and (3) utility can be unravelled with ease from this disentangled or loosely twisted end. That said, these terms, as part of the objective function, exert in-

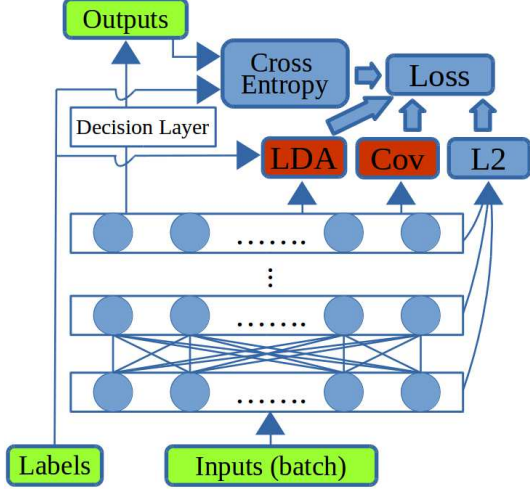


Figure 1: Pushing Step. Our deep LDA push objectives are colored in red. They maximize, unravel, and condense useful information flow transferred over the network and bring discriminants into alignment with latent space neurons. L_2 regularization is also applied to the decision layer, but is not shown for clarity.

fluence over the whole network. Next, we will provide more details about the above-mentioned pushing objectives and show how they maximize and push class separation utility into alignment with latent space neurons.

Apart from cross-entropy and L_2 losses, we explicitly and proactively apply linear discriminant analysis in the final latent space to maximize class separation. The goal of the LDA term is to transform data from a noisy and complicated space to one where different categories can be linearly separated apart (there is only one final FC layer left). It is aligned with the training goal to reduce classification error. Latent features learned are expected to pick up class separating statistics in the input. Inspired by [9, 48], we define our deep LDA utility for classification as the ratio of between-class scatter to within-class scatter in the final latent space.

$$S_{W,\theta} = \frac{|W^T \Sigma_{b,\theta} W|}{|W^T \Sigma_{w,\theta} W|} \quad (1)$$

where

$$\Sigma_{w,\theta} = \sum_i \tilde{X}_{\theta,i}^T \tilde{X}_{\theta,i} \quad (2)$$

$$\Sigma_{b,\theta} = \Sigma_{a,\theta} - \Sigma_{w,\theta} \quad (3)$$

$$\Sigma_{a,\theta} = \tilde{X}_{\theta}^T \tilde{X}_{\theta} \quad (4)$$

with $X_{\theta,i}$ being the set of observations obtained in the final latent space for category i , with model parameter setting θ .

A pair of single vertical bars denotes matrix determinant. The tilde sign ($\tilde{\cdot}$) represents a centering operation; for data X this means:

$$\tilde{X} = (I_n - n^{-1} \mathbf{1}_n \mathbf{1}_n^T) X \quad (5)$$

where n is the number of observations in X , $\mathbf{1}_n$ denotes an $n \times 1$ vector of ones. The training objective of deep LDA is to maximize the final latent space class separation (Eq. 1), which comes down to solving the following generalized eigenvalue problem:

$$\Sigma_{b,\theta} \vec{e}_j = v_j \Sigma_{w,\theta} \vec{e}_j \quad (6)$$

where (\vec{e}_j, v_j) represents a generalized eigenpair of the matrix pencil $(\Sigma_{b,\theta}, \Sigma_{w,\theta})$ with \vec{e}_j as a W column. The LDA objective can be achieved by maximizing the average of v_j s. Thus, we define the LDA-related loss term as its reciprocal:

$$\ell_{lda} = \frac{N}{\sum_i v_j} \quad (7)$$

Simultaneously, to penalize co-adapted structures and reduce redundancy in the network, we inject covariance penalty into the latent space. The corresponding loss is:

$$\ell_{cov} = \|\Sigma_{a,\theta} - \text{diag}(\Sigma_{a,\theta})\|_1 \quad (8)$$

where $\|\cdot\|_1$ indicates entrywise 1-norm. This term agrees with the intuition that, unlike lower layers' common primitive features, higher layers of a well-trained deep net capture a wide variety of high-level, global, and easily disentangled abstractions [3, 64]. Generally speaking, the odds of various high-level patterns firing together should be low. As a side effect, ℓ_{cov} encourages weights/activation to be zero and thus reduce over-fitting. This is similar to what dropout and L_1/L_2 regularization do during training, but in a non-random and activation-based way.

Furthermore, in order to prune on the neuron level without much information loss, we need to align the above mentioned LDA utility (v_j s) with neuron dimensions. For this purpose, we try to align W columns with standard basis directions and let the network learn an optimal θ that leads to large class separation. This will also save us from using an actual W rotation in addition to a neural net. Given that duplicate neurons have been discouraged by ℓ_{cov} and inactive neurons are not considered here, Eq. 6 can be rewritten as:

$$(\Sigma_{w,\theta}^{-1} \Sigma_{b,\theta}) \vec{e}_j = v_j \vec{e}_j \quad (9)$$

As we can see, W column \vec{e}_j s are the eigenvectors of $\Sigma_{w,\theta}^{-1} \Sigma_{b,\theta}$. Thus, forcing the direction alignment of LDA utilities and neuron dimensions is equivalent to forcing $\Sigma_{w,\theta}^{-1} \Sigma_{b,\theta}$ to be a diagonal matrix. We incorporate this constraint by putting the following term to the loss function:

$$\ell_{align} = \left\| \Sigma_{w,\theta}^{-1} \Sigma_{b,\theta} - \text{diag}(\Sigma_{w,\theta}^{-1} \Sigma_{b,\theta}) \right\|_1 \quad (10)$$

where, similar to Eq. 8, entrywise 1-norm is used instead of entrywise 2-norm (a.k.a. Frobenius norm) because our aim is to put as many off-diagonal elements to zero as possible. Putting all terms together, we get our pushing objective as follows. Its three components jointly maximize class separation, squeeze, and push classification utility into a compact set of neurons for later pruning:

$$\ell_{push} = \gamma \ell_{lda} + \lambda \ell_{cov} + \beta \ell_{align} \quad (11)$$

where λ , β , and γ are weighting hyperparameters. They are set so that (1) LDA utilities and neuron dimensions are aligned and (2) a high accuracy is maintained. In our experiments, through network parameter θ learning, the two goals can actually be met simultaneously. In fact, the pushing terms lead to higher accuracy than just using cross entropy and L_2 regularization on all the three datasets in our experiments (details in Sec. 5). In addition to class separation utility boost, another possible reason is that the extra constraints of our deep LDA pushing terms (Eq. 11) can add some structure/regularization to the original overfitted deep space with very high degree of freedom. These terms help constrain useful information within or near more compact manifolds. It is worth mentioning that ℓ_{lda} is sometimes numerically unstable. Inspired by [11], we add a multiple of the identity matrix to the within scatter matrix. Also, when the category number is large (e.g., 1000 for ImageNet), it is hard to include all categories in one forward pass. In our implementation, the scatter matrices at a certain batch are calculated for a random subset of classes. Each class is set to have the same (or similar) number of samples (≥ 8). This approximation strategy fits well with the stochastic nature of the training. When latent space dimension d is large (e.g., in the first iteration), the ℓ_{align} constraint which includes an expensive $d \times d$ matrix inverse operation can be lifted. The reason is that in the context of over-parameterized network and high dimensional latent space, neuron activation is sparse: only a limited number of neurons tend to fire for a class and each high-level neuron motif corresponds to only one or few classes. In this scenario, positive within-class correlation indicates positive total correlation, and minimizing ℓ_{cov} has an effect of minimizing ℓ_{align} . Through training with the pushing objectives added, the network learns to organize itself in an easily pruned way. W columns that maximize the class separation (Eq. 1) are expected to be aligned with (some of) the original neuron dimensions. Since cross entropy and L_2 regularization have been widely adopted in deep network training, we will skip the details of the two terms. This pushing step lays the foundation for neuron/filter level pruning across all layers.

3.2. Pruning Step

After the pushing step, the final class separation power is maximized and simultaneously pushed into alignment with

top layer neurons. It follows that the direct abandonment of less useful neurons and their dependencies on previous layers is safe. The discriminant power along the j th neuron dimension v_j is the corresponding diagonal value of $\Sigma w^{-1} \Sigma_b$:

$$v_j = \text{diag}(\Sigma w^{-1} \Sigma_b)_j \quad (12)$$

We treat pruning as a dimensionality reduction problem in the deep feature space. When pruning, we discard neuron dimension js of small v_j along with its cross-layer contributing sources in the ‘pushed’ model where useful components have been separated from others. This step is illustrated as Figure 2. For modular structures, the idea is the same except that we need to trace dependencies, i.e. apply deconvolution, for different scales in a group-wise manner.

Deconvolution (deconv) is often used in signal processing to reverse unknown filters’ effect and recover corrupted sources [18]. Inspired by this, we trace the classification utility unravelled from final latent space backwards across all layers via deconvolution. In the final layer, only the most discriminative dimensions’ response is preserved (other dimensions are set to 0) before deconv starts. It is worth mentioning that ‘deconvolution’ can be a confusing term today. Here we employ the same deconv utility tracing as in [62], which is based on [64]. One difference is that Zeiler and Fergus [64] use ‘deconvolution’ for visualization purposes in the image space while we focus on reconstructing contributing sources over the layers. Also, the proposed method only back-propagates useful final variations. Irrelevant and interfering features of various kinds are ‘filtered out’. As an inverse process of convolution, the unit deconv procedure performs convolution with the same filters transposed. It can be considered as inversion of convolution with an orthogonal assumption about the convolution matrix.

$$U_i = F_i^T Z_i \quad (13)$$

Over the layers (ignoring nonlinearity and unpooling),

$$Z_{i-1} = U_i \quad (14)$$

where i indicates a layer, U_i and Z_i are layer i input and output features with components not contributing to final utility removed. The l th columns of U_i and Z_i are respectively converted from layer i reconstructed useful inputs and outputs w.r.t. input image l . Further details of the deconv utility tracing can be found in [62]. With all neurons’/filters’ utility for final discriminability known, pruning simply becomes discarding structures that are less useful to final classification (e.g. structures colored white in Fig 2). For this purpose, we use a standard deviation based thresholding strategy to quickly get rid of massive less informative neurons while being cautious in high utility regions (at high

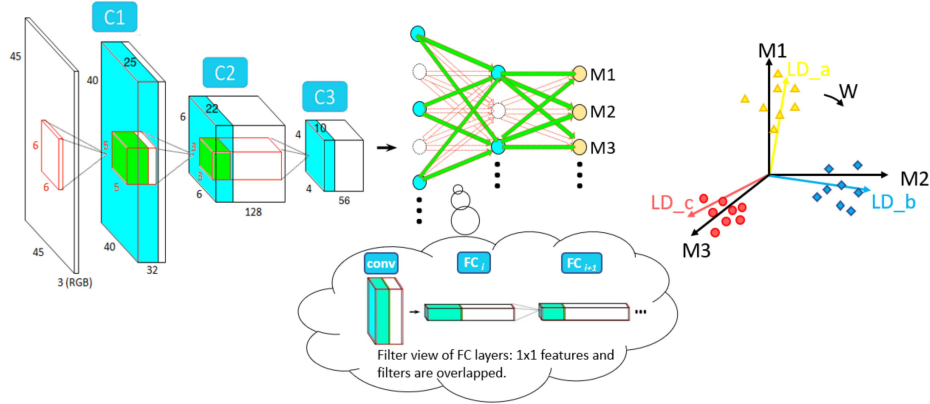


Figure 2: Depiction of neuron or filter level LDA-Deconv utility tracing. Useful (cyan) neuron outputs/features that contribute to final deep LDA utility through corresponding (green) next layer weights/filters, only depend on previous layers’ (cyan) counterparts via deconv. White denotes useless components. W is defined in Equation 1. M indicates final latent space neuron dimensions. The bubble cloud explains how deconv can be applied to FC layers. Each FC neuron is a stack of 1×1 filters with one 1×1 output feature map.

percentiles). The threshold is directly related to the pruning rate. Since feature maps (neuron outputs) correspond to next-layer filter depths (neuron weights), our pruning leads to filter-wise and channel-wise savings simultaneously. After pruning at each iteration, retraining with surviving parameters is needed.

4. Compact architecture search

Pruning can be considered as an architecture search process. The main drawback is that the top-down, one-way search is bounded above by the base net’s capacity. For datasets requiring larger capacities than the base net can offer, a growing step before iterative push-and-prune would be necessary to first encompass and contain enough task-desirable architecture candidates. In the language of the famous ‘lottery ticket hypotheses’ [10], the growing step’s effect is equivalent to ‘buying more lottery tickets’ so that the chance for getting a winning ticket is boosted. In this section, we propose a simple but effective growing step based on the Inception module which can be easily combined with our deep LDA pruning.

4.1. Starting base structure

In this subsection, we explore the building block options for the growing procedure and discuss their advantages and disadvantages for our purpose of deriving task-desirable compact architectures. The discussions are grouped under the following topics.

4.1.1 Inception v.s. Residual modules

In the deep learning literature, two of the most popular convnet modules are Inception modules [58] and Resid-

ual modules [19]. We prefer the Inception module over ResNets’ residual modules because the latter has hard-coded dimension alignment. The skip/residual dimension has to agree with the main trunk dimension for summation. However, after pruning according to any importance measure (including ours), they do not necessarily agree unless we force them to. Given that each ResNet module has only 2-3 layers, such a hard-coded constraint at every module end would greatly limit the freedom of pruning. That said, summation as in a residual module is more efficient than Inception module’s concatenation for very deep networks as summation greatly reduces output feature maps’ depth. Since our final goal is to boost efficiency via pruning, we do not care much about this during the base net growing stage. Another reason why we prefer the Inception module is that, compared to residual models, inception modules offer us a variety of filter types. Our deep LDA pruning can take advantage of this by selecting both the numbers and types of filters on different abstraction levels.

It has been proven that deep networks are able to approximate the accuracy of shallow networks with an exponentially fewer number of parameters, at least for some classes of functions [59, 8, 39, 53, 45]. One fundamental breakthrough of ResNet is that it allows people to train extremely deep neural networks with up to hundreds of layers successfully. Compared to ResNet, current Inception models have only a dozen or so modules. In this paper, we explore to grow from the basic inception net [58] by greedily stacking more unit modules and see whether the resulting deep Inception nets can achieve ResNet-comparable accuracy.

4.1.2 Original Inception v.s. later variants

We use the initial Inception net (a.k.a. GoogLeNet) as the starting point but with two modifications inspired by [30]. The first is to approximate the function of 5×5 filters with two consecutive 3×3 filters, and the second is to add batch normalization after each conv layer. In the rest of the paper, when we talk about the Inception module or net, we refer to this variant. Later inception modules (V2-V4) include more architecture fiddling and usually require higher resolution data (299×299 rather than 224×224). We do not incorporate those changes since we want to perform fair comparisons between our grown deep Inception nets and ResNets as well as some other popular networks taking 224×224 images as input. Also, this keeps human expert knowledge involved as minimum as possible. Ideally, we aim to replace such human knowledge with learning and pruning.

Interestingly, despite the simplicity, no works have investigated the possibility of simply growing from the original Inception net. BN-GoogLeNet is proposed in [30], but it is not just GoogLeNet with batch normalization. Compared to the very first Inception net version, filter and module numbers in BN-GoogLeNet are actually increased. As a consequence, it is much larger in size. To our knowledge, there is no explicit justification so far why this architecture change is desirable or necessary. In this paper, we attempt to fill this gap and explore the possibility of boosting accuracy via simply adding more Inception modules before our deep LDA based pruning.

4.2. Greedy base network growing strategy

We grow deep Inception nets by greedily and iteratively stacking more modules. This base net growing strategy can be viewed as a simple trial-and-error evolutionary algorithm, which is demonstrated as Algorithm 2.

At each iteration, we try to add one module to one of the network stages. Here, a stage consists of several modules before a pooling layer with the same output feature map dimension. For example, there are three stages in the original Inception net after the stem layers, with respectively 28×28 , 14×14 , 7×7 output feature map sizes. The newly added module has the same architecture as the module underneath. We quickly train all the possible options (e.g., 3 for the Inception net) and keep only the one that achieves the highest accuracy. The process is repeated for N iterations until reaching a complexity bound (e.g., memory limit) or until no noticeable accuracy gain can be observed after two consecutive iterations. Like the initial Inception net, when training, two auxiliary classifiers are added to the second stage (one after the first module and the other before the last module). We find the auxiliary classifiers very useful when the depth becomes large. A long warm-up phase can also be helpful. By this growing strategy, a superset of abundant deep features can be obtained, from which deep LDA push-

Algorithm 2: Greedy base net growing strategy

Input: $net = \{s_0, s_1, \dots, s_i, \dots\}$, $s_i = \{m_{i0}, m_{i1}, \dots, m_{ij}, \dots\}$, where s : stage, m : module, net : starting base. N : number of extra modules to add

Output: net with N extra modules added

$n = 1$; $acc_{max} = 0$; net_{opt}

while $n \leq N$ **do**

for stage **in** net **do**

$net' = extend(net, stage)$

 train net' and predict, get val accuracy acc

if $acc > acc_{max}$ **then**

$acc_{max} = acc$

$net_{opt} = net'$

end

end

$net = net_{opt}$, save if necessary

$n = n + 1$

end

return net

ing and pruning can locate or derive task-desirable ones (a ‘besiege-and-hunt’ process).

4.3. Deep Inception nets

Table 1 shows some models encountered in the above-mentioned growing process using the basic Inception module on the ImageNet dataset. The accuracy in Table 1 is Top-1 accuracy using only one center crop. The name Inception- N means the net is N -layer deep (only conv and fully-connected layers are considered).

According to the results, we can see that more accuracy can be obtained by simply stacking more modules and that very deep inception nets can achieve ResNet-level accuracy without hard-coded dimension alignment by human experts. Specifically, we would like to introduce Inception-88, a deep Inception net with 25.1M parameters that achieves 75.01% top-1 accuracy on ImageNet using 1-crop validation (highlighted in Table 1). This 88-layer deep model is similar in both size and accuracy to ResNet-50 which has a total of 25.5M parameters and achieves 74.96% top-1 accuracy on ImageNet. Beyond Inception-88, accuracy first drops slightly before increasing slowly with the increase of module number. This is also similar to the ResNet-50 case where 19M more parameters (ResNet-101) result in only about 1% accuracy gain (76.2% vs. 75.0%) in our experiments on ImageNet. More details about Inception-88 can be found in Appendix A. The depths of the three stages are respectively 30, 24, and 30.

Inception-88 is not just another handcrafted architecture. As mentioned previously, ResNets are not very pruning-

Name	Modules	Stage size	Parameters	FLOPs	Accuracy
InceptionV1	9	(2,5,2)	6.7M	3.0B	70.64%
Inception-34	10	(3,5,2)	7.1M	3.7B	71.12%
Inception-37	11	(3,5,3)	8.6M	3.8B	71.75%
Inception-40	12	(4,5,3)	9.0M	4.5B	71.97%
Inception-43	13	(4,6,3)	10.0M	4.9B	72.03%
Inception-46	14	(4,7,3)	11.0M	5.3B	73.45%
Inception-49	15	(4,7,4)	12.5M	5.4B	73.51%
Inception-52	16	(4,7,5)	14.0M	5.6B	73.69%
Inception-55	17	(4,8,5)	15.0M	6.0B	73.91%
Inception-58	18	(5,8,5)	15.5M	6.6B	74.27%
Inception-61	19	(6,8,5)	15.9M	7.3B	74.20%
Inception-64	20	(7,8,5)	16.3M	8.0B	74.42%
Inception-67	21	(7,8,6)	17.8M	8.1B	74.58%
Inception-70	22	(7,8,7)	19.3M	8.3B	74.54%
Inception-73	23	(8,8,7)	19.8M	8.9B	74.64%
Inception-76	24	(8,8,8)	21.3M	9.1B	74.60%
Inception-79	25	(8,8,9)	22.8M	9.2B	74.59%
Inception-82	26	(9,8,9)	23.2M	9.9B	74.77%
Inception-85	27	(9,8,10)	24.7M	10.1B	74.60%
Inception-88	28	(10,8,10)	25.1M	10.7B	75.01%
Inception-91	29	(10,8,11)	26.6M	10.9B	74.71%

Table 1: Deep Inception net examples encountered in the base net growing process on ImageNet. The accuracy here indicates Top-1 accuracy using only one center crop. The name Inception-N means the net is N -layer deep (only conv and fully-connected layers are considered). The stage size column shows module numbers across the three stages. M= 10^6 , B= 10^9 .

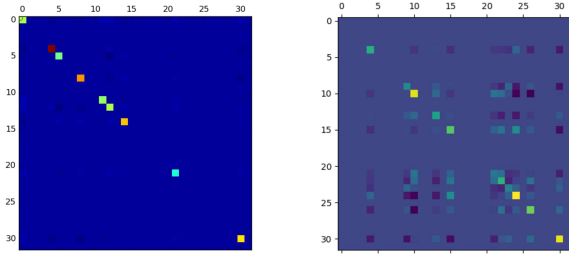
friendly, and the hard-coded dimension alignment is fragile to pruning. With Inception-88, we achieve comparable accuracy to ResNet-50 at a similar complexity while no dimension constraints are imposed. Thus, we hope that this architecture can provide pruning algorithms with more freedom. Such freedom is especially important to our deep LDA pruning that performs dimension reduction in the deep feature space. Combining the growing step with previously presented deep discriminant analysis based pushing and pruning, we achieve a feasible pipeline for compact architecture search. Compared to many expensive NAS approaches that may take several weeks on hundreds of GPUs, our pipeline has several advantages. One is that rather than sampling a great many architectures (out of infinite possibilities), our top-down search only needs to sample along the direction that is aligned with task utility. Due to the limited number of sampled architectures, we do not need to approximate or predict sampled architectures’ performance. Instead, we can simply retrain all the sampled (pruned) architectures to obtain accurate evaluations. Even better, useful parameters inherited from the previous base make the sample architecture retraining process converge fast.

5. Experiments and results

This section tests our proactive deep discriminant analysis based pruning on the MNIST, CIFAR10, and ImageNet datasets. We only perform push and prune on the first two datasets while apply the whole grow-push-prune architecture search pipeline on ImageNet. It is worth mentioning that there are various techniques and tricks in addition to architecture that may help increase the absolute accuracy numbers, such as more advanced optimization strategies, decay policies, multicropping, label smoothing regularization, mixup training, distillation, and so on [21]. We did not use such tricks because our focus is not the absolute accuracy value but rather its change with pruning. Also, most of the tricks mentioned above are designed on ImageNet, and they may not transfer well to other datasets.

5.1. A toy experiment on MNIST

MNIST [34] is a dataset of handwritten digits where each image is a 28×28 grayscale image representing the digits 0-9. The dataset consists of 60,000 training images and 10,000 test images. We leave out the first 1,000 images in each category of the training set for validation purposes. With a simple five hidden layer fully-connected network (1024-1024-1024-1024-32), we will show deep LDA push-



(a) with pushing objective (b) without pushing objective

Figure 3: Variance-covariance matrices of the latent space neuron output after training (a) with and (b) without the pushing objective (Sec. 3.1) on the MNIST dataset using a toy FC architecture (hidden dimensions: 1024-1024-1024-1024-32). The values are color coded using the default bgr color map of the Matplotlib pyplot matshow function [28]. From small to large values, the color transits from blue to green and finally to red.

ing’s efficacy. In this toy experiment, the last hidden layer is set to have 32 neurons simply for illustration clarity.

5.1.1 Deep LDA pushing’s influence on the latent space

As mentioned previously, the main purpose of proactive LDA pushing (Sec. 3.1) is to push deep discriminants or class separation power into alignment with latent space neuron dimensions so that filter-level pruning is safe. Although the pushing influence is across the layers, here via this toy example, we only illustrate how the final latent space is changed as other layers’ changes influence the final decision via this space. Figure 3 visualizes the variance-covariance matrix of latent space neuron output after training with and without the pushing objective.

From Fig. 3, we can see that our proposed deep LDA pushing objective is effective and it successfully pushes useful final decision-making variances to a subset of latent space neuron dimensions. Compared to Fig. 3b, training with the pushing objective better decorrelates useful variances (Fig. 3a). As mentioned previously, this contributes to the alignment of deep discriminants with latent space neuron dimensions. Most importantly, the accuracy does not change much by including the deep LDA pushing objective in the cost function. In fact, the accuracy even improves a little with the pushing objective added. In our experiments, the conventional cross-entropy with L_2 regularization leads to an accuracy of 97.9% on the validation set. This number increases to 98.3% with the addition of the deep LDA pushing objective.

Figure 4 shows the top nine discriminants after training with and without our pushing objective. As expected, the

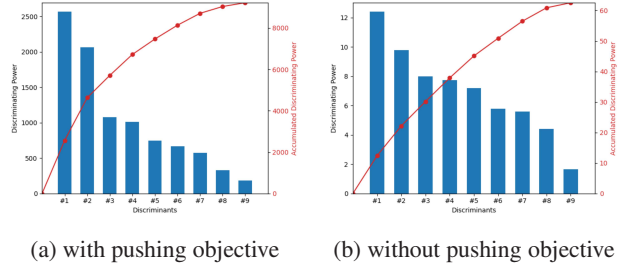


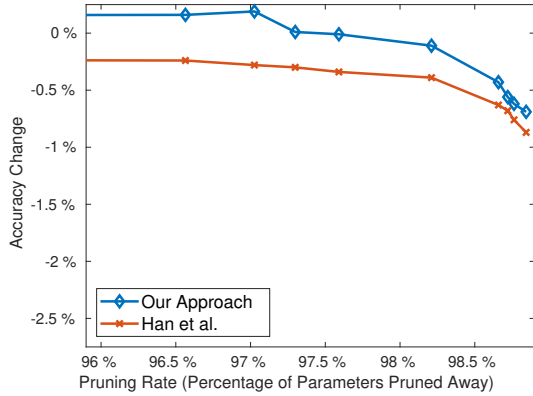
Figure 4: Top nine discriminants after training (a) with and (b) without our pushing objective. The horizontal axis represents the nine top discriminants and the left vertical axis indicates their corresponding discriminating power (v_j in Eq. 9 and Eq. 12). The right vertical axis and the curve in red denote the accumulated discriminating power.

discriminating power, i.e., v_j in Eq. 9 and Eq. 12, is improved with our deep LDA pushing by two orders of magnitude. Also, the distribution after pushing is more spiky and, in terms of proportion, more discriminating power is pushed to the large discriminants on the left. This can be seen from the red accumulative discriminating power curve in Fig. 4a and 4b. The first two discriminants count for 35% of the nine discriminants’ total power in Fig. 4b while this number increases to 50% for the case with our pushing objective. When pruning, it means that we can throw away more neuron dimensions while still maintaining enough discriminating power. In this simple example, all neurons other than the top nine are put to dormant (with 0 discriminating power) after our pushing while there are a few more neurons (with small positive or even negative discriminants) in the no-push case. These neurons are not included in Figure 4.

5.1.2 Accuracy change v.s. parameters pruned

Figure 5 illustrates the relationship of accuracy change v.s. parameters pruned on the validation set. Weight magnitude based pruning (Han *et al.* [16]) is included as a comparison to ours. For this toy experiment, we only prune the network in one iteration. Low pruning rates are skipped where accuracy does not change much.

As we can see from Figure 5, both pruning approaches lead to high pruning rates while maintaining accuracies comparable to the original. The high pruning rates are mainly due to the MNIST dataset’s simplicity and the heavy fully-connected architecture. As anticipated, our deep LDA based pruning enjoys higher accuracy at similar complexities than [16]. Here, the gap becomes smaller when the pruning rate is high. The main reason is that the pruning is done noniteratively. Aggressive pruning in one shot renders utility recovery via re-training more difficult. With more and more parameters discarded in one shot, the value con-



MNIST, base accuracy: 97.9%, after pushing: 98.3%

Figure 5: Accuracy change vs. parameters savings of our method (blue) and Han *et al.* [16] (red) on MNIST. The pruning is done in one iteration. Small pruning rates are skipped where accuracy does not change much.

Methods	MNIST	
	Acc	Param#
Base net	98.1%	4.0M
Han <i>et al.</i> [16]	96.9%	38.6K
Our Pruned net	97.6%	38.6K

Table 2: Testing accuracies on MNIST. Acc: test set accuracy, Param#: the number of parameters. $M=10^6$, $K=10^3$.

tained in the remaining weights decreases gradually, and so does its advantage over simple weights based pruning. Table 2 shows the test set performance. The smallest deep-LDA pruned network in our experiments with comparable accuracy to the original is selected (accuracy loss within 1%). The testing accuracy of one network pruned by [16] at a similar complexity is also reported.

5.2. CIFAR10

CIFAR10 [33] is composed of 60,000 32x32 color images from 10 classes, i.e., airplane, automobile, bird, cat, deer, dog, frog, horse, ship, truck. In total, there are 50,000 training images and 10,000 testing images. We use the first 10,000 images in the training set for validation purposes.

5.2.1 Accuracy change v.s. pruning rate

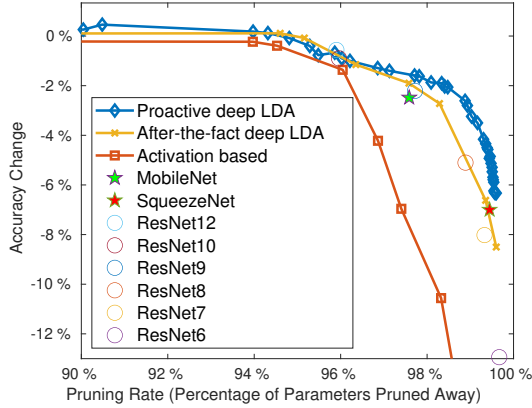
In this experiment, we start with a VGG-16 model pre-trained on ImageNet. Cross-entropy loss with L_2 regularization leads to a validation accuracy of 95.19% on CIFAR10. In addition to aligning discriminants with neuron dimensions, our deep LDA pushing objective helps improve the accuracy to 95.72% without pruning. Figure 6 illustrates the change of accuracy with respect to param-

Name	Configuration
ResNet6	i64-c128
ResNet7	i64-c128-1c256
ResNet8	i64-c128-c256
ResNet9	i64-c128-c256-1c512
ResNet10	c64-c128-c256-c512
ResNet12	(c64, i64)-c128-c256-c512

Table 3: Tiny ResNets used as comparison in our experiments on CIFAR10. The dash sign ‘-’ separates different stages. As defined in [19], there are two types of residual modules, i.e., identity module and convolutional module where 1×1 filters are employed on the shortcut path to match dimension. Only depth-2 modules are used here. In this table, ‘i’ stands for depth-2 identity block and ‘c’ represents depth-2 convolutional block. The number follows ‘i’ or ‘c’ indicates the number of filters within each conv layer in that module. Parentheses are used to group multiple modules in a stage. In addition to residual modules, we adopt the same stem layers as in [19].

ters pruned away. We focus on high pruning rates where the accuracy changes fast with the decrease of parameters. That said, it is worth noting that among the few small pruning rates investigated, a pruned model with 118M parameters enjoys an even better accuracy (96.01%) than both the original model and the pushed one. For comparison, we add after-the-fact deep LDA pruning [62] and activation-based filter pruning (as mentioned in [42]), which treats filter importance as average activation magnitudes/variances within a filter. Also, we compare our method with some popular compact fixed nets, i.e., MobileNet [26], SqueezeNet [29], and tiny ResNets. Here, tiny ResNets refer to residual nets with shallow depths. In this experiment, we test ResNet12, ResNet10, ResNet9, ResNet8, ResNet7, and ResNet6. Their detailed configurations are shown in Table 3.

As we can see from the results, our proactive-deep-LDA pruning, generally speaking, enjoys higher accuracy than the other two pruning approaches and the compact nets at similar complexities. The gaps are more obvious at high pruning rates, especially between activation-based pruning and our proactive deep LDA pruning. This performance difference implies that strong activation does not necessarily indicate high final classification utility. It is possible that some strong yet irrelevant activation skews or misleads the data analysis at the top of the network. Compared to after-the-fact deep LDA pruning [62], the proactive deep LDA pruning proposed in this paper enjoys a better performance, especially at the high end of the pruning rate spectrum. The reason is that although after-the-fact deep LDA is capable



CIFAR10, base acc.: 95.19%, after pushing: 95.72%

Figure 6: Accuracy change v.s. parameters savings on CIFAR10. In addition to our proactive deep LDA pruning, we add after-the-fact deep LDA pruning [62], activation-based pruning (as mentioned in [42]), MobileNet [26], SqueezeNet [29], and tiny ResNets for comparison. Tiny ResNets configurations are shown in Table 3. Small pruning rates are skipped where accuracy does not change much.

of capturing final class separation utility, useful and useless components may already be mixed in the given pre-trained model, and it is hard to trim one without influencing the other. The performance differences are small at low pruning rates, perhaps because even when ‘useful’ feature components are discarded, the network can recover such or similar features through re-training when pruning rates are low. This ‘learning to repair’ ability via re-training gradually declines when the network capacity becomes small. Furthermore, even though ResNet is one of the most successful deep nets in the literature, stacking a few residual modules with random numbers of filters only leads to sub-optimal performance compared to the proposed proactive deep LDA pruning. In Figure 6, our deep LDA-pushed-and-pruned models beat tiny ResNets at most similar complexities. This indicates the necessity of informed pruning/architecture search over architecture hand-engineering with human expertise.

5.2.2 Layerwise complexity

Figure 7 demonstrates the layerwise complexity of our smallest pruned model that maintains comparable accuracy to the original VGG-16. FC layers dominate the original net size, while almost all computation comes from conv layers. According to the results, most parameters and computations have been thrown away in the layers except for the first three layers that capture commonly useful patterns.

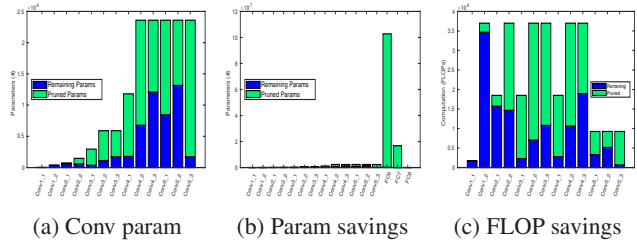


Figure 7: Layerwise complexity reductions (CIFAR10, VGG16). Green: pruned, blue: remaining. We add a separate parameter analysis for conv layers because FC layers dominate the model size. Since almost all computations are in the conv layers, only conv layer FLOPs are demonstrated.

5.3. ImageNet

In this subsection, we demonstrate our ‘grow-push-prune’ pipeline’s efficacy on the ImageNet dataset. ImageNet is a popular dataset that contains over 1.28M training images and 50K validation images. It is widely used for benchmarking algorithms in computer vision and machine learning. In our experiment, all the images are pre-resized to 256x256. During training, the images are randomly cropped to 224x224 and randomly mirrored about the vertical axis. No bounding box information is used. Following the practice of most previous pruning works on ImageNet, we report accuracy change directly on the validation set using the center crop (no labelled test split is publicly available).

In Sec. 4.3, through growing from the basic InceptionV1, we obtain an Inception-88 model that achieves comparable accuracy to ResNet-50 at a slightly smaller complexity on ImageNet. Apart from increasing capacity and accuracy, this growing step offers more room for the net to stretch and adjust itself at the next pushing step. After the growing step, we perform deep LDA pushing and pruning on the Inception-88 model to separate and strip off unnecessary complexities. In this way, bottom-up search and top-down search are combined.

5.3.1 Accuracy change v.s. pruning rate

In Figure 8, we compare our ‘grown-pushed-pruned’ models with the deep Inception nets derived from the growing step, a range of residual architectures at different complexities, and some popular fixed nets (i.e., SqueezeNet [29], MobileNet [26], BN-GoogLeNet¹ [30]). We also include the results of training some of our pruned architectures from scratch. These architectures only duplicate the structures of

¹BN-GoogLeNet [30] is not just GoogLeNet with batch normalization. There are more architectural changes to InceptionV1 which we do not include in our grown deep Inception nets.

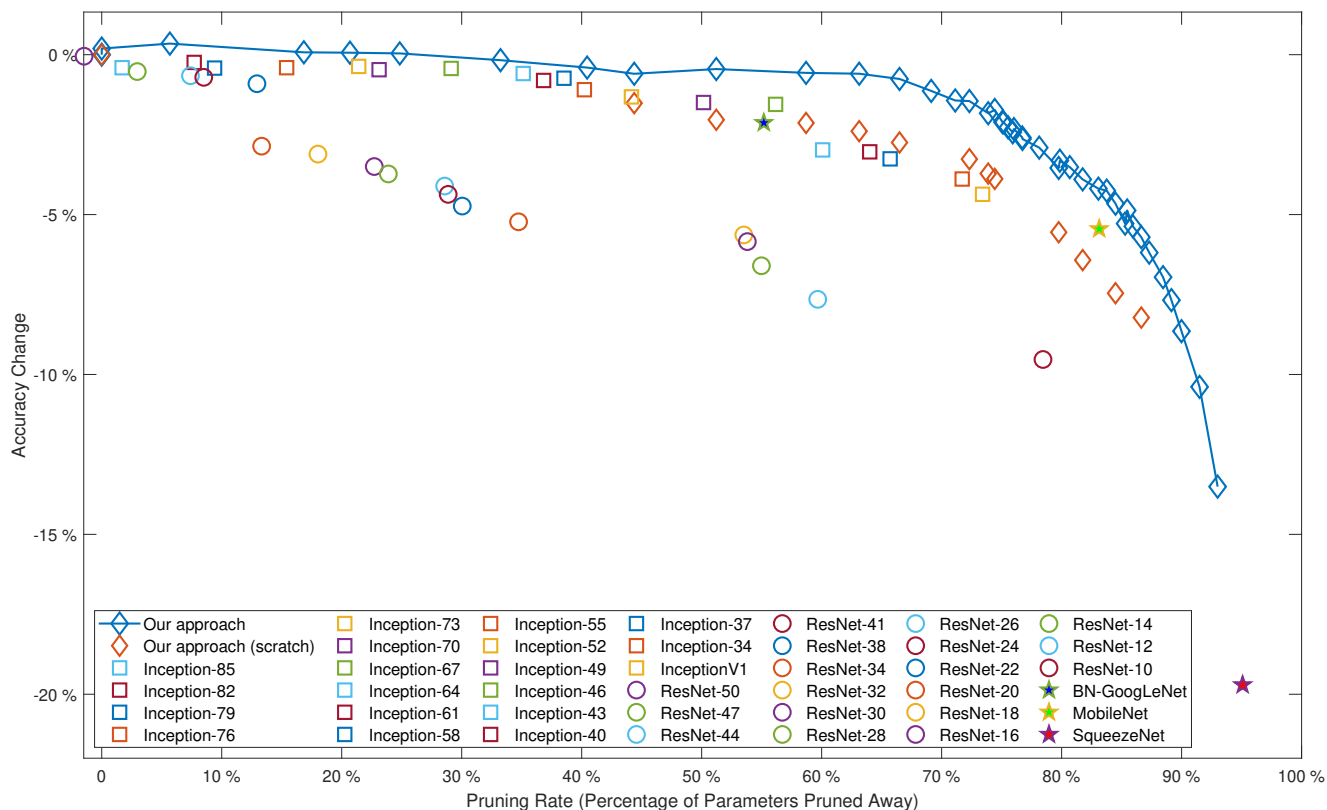


Figure 8: Accuracy change vs. parameters savings on ImageNet. In addition to our deep LDA push-and-prune method (blue), we add our grown deep Inception nets (details in Table 1), ResNets at different complexities (configurations in Table 4), BN-GoogLeNet [30], MobileNet [26], SqueezeNet [29] for comparison. In fact, there are two accuracies when pruning rate is 0. The lower one indicates Inception-88 trained with only cross-entropy and L_2 losses while the upper one represents the same architecture trained with our deep LDA push objective added. The negative pruning rate of ResNet-50 means that ResNet-50 has more parameters than our Inception-88 base. Our derived nets trained from scratch (red diamonds) mark the beginning of each iteration for our approach.

our pruned models at the beginning of each iteration, but no weights are inherited either directly or indirectly from the base model. The detailed configurations of the ResNets used for comparison are shown in Table 4. Starting from ResNet-50, each time a residual module is removed from the stage with the most modules. When two stages have the same number of modules, we follow a bottom-to-top order to choose which module to remove (until ResNet18). From ResNet-50 to ResNet-38, the residual modules are of depth 3. From ResNet-34 downwards, each module has a maximum depth of 2. The depth-2 and depth-3 residual modules are defined in [19].

According to Figure 8, we can see that our compact models pushed-and-pruned from Inception-88 beat both smaller deep Inception nets and the residual architectures at similar complexities. The gaps are more obvious at large pruning rates. This demonstrates the proposed grow-push-

prune pipeline’s efficacy, and it further strengthens our confidence in deep LDA based pruning and architecture search. Our pruned models achieve better performance compared to training the same architectures from scratch. This highlights the value of the knowledge acquired by and transferred from the larger grown base model in the form of weights. That said, even when trained from scratch, our pruned nets still attain satisfactory accuracy and beat others when the pruning rate is above 55% (one exception is MobileNet, which employs depthwise separable convolution to help reduce complexity further). It means that, besides the weights, there is some value in the pruned architecture itself. When retraining with inherited weights, the pruned models converge much faster than training from scratch. Usually, it only takes a few epochs to achieve accuracy within 5% from that of the fully trained. This makes our pipeline a practical alternative to expensive NAS methods

Name	Configuration
ResNet6	i64-c128
ResNet7	i64-c128-1c256
ResNet8	i64-c128-c256
ResNet9	i64-c128-c256-1c512
ResNet10	c64-c128-c256-c512
ResNet12	(c64, i64)-c128-c256-c512
ResNet18	(c64, i64)-(c128, i128)-(c256, i256)-(c512, i512)
ResNet20	(c64, i64)-(c128, i128)-(c256, i256)-(c512, i512, i512)
ResNet22	(c64, i64)-(c128, i128)-(c256, i256, i256)-(c512, i512, i512)
ResNet24	(c64, i64)-(c128, i128, i128)-(c256, i256, i256)-(c512, i512, i512)
ResNet26	(c64, i64, i64)-(c128, i128, i128)-(c256, i256, i256)-(c512, i512, i512)
ResNet28	(c64, i64, i64)-(c128, i128, i128)-(c256, i256, i256, i256)-(c512, i512, i512)
ResNet30	(c64, i64, i64)-(c128, i128, i128, i128)-(c256, i256, i256, i256)-(c512, i512, i512)
ResNet32	(c64, i64, i64)-(c128, i128, i128, i128)-(c256, i256, i256, i256, i256)-(c512, i512, i512)
ResNet34	(c64, i64, i64)-(c128, i128, i128, i128)-(c256, i256, i256, i256, i256, i256)-(c512, i512, i512)
ResNet38	(C64, I64, I64)-(C128, I128, I128)-(C256, I256, I256)-(C512, I512, I512)
ResNet41	(C64, I64, I64)-(C128, I128, I128)-(C256, I256, I256, I256)-(C512, I512, I512)
ResNet44	(C64, I64, I64)-(C128, I128, I128, I128)-(C256, I256, I256, I256)-(C512, I512, I512)
ResNet47	(C64, I64, I64)-(C128, I128, I128, I128)-(C256, I256, I256, I256, I256)-(C512, I512, I512)
ResNet50	(C64, I64, I64)-(C128, I128, I128, I128)-(C256, I256, I256, I256, I256, I256)-(C512, I512, I512)

Table 4: ResNets used as comparison in our experiments on ImageNet. The dash sign ‘-’ separates different stages. As defined in [19], there are two types of residual modules, i.e., identity module and convolutional module where 1×1 filters are employed on the shortcut path to match dimension. Here, ‘i’ stands for depth-2 identity block, ‘c’ represents depth-2 convolutional block, ‘I’ stands for depth-3 identity block, and ‘C’ represents depth-3 convolutional block. The number follows ‘i’, ‘c’, ‘I’, or ‘C’ indicates the number of filters within each conv layer in that module. Parentheses are used to group multiple modules in a stage. In addition to residual modules, we adopt the same stem layers as in [19].

that train a large number of architecture samples separately or based on some ad hoc relations.

It is worth noting that the Inception-88 net achieves 75.01% accuracy after training only with cross-entropy and L_2 losses. Adding the proposed deep LDA pushing terms in the objective increases the accuracy number to 75.2%, in addition to aligning utility with latent neuron dimensions. At the pruning rate of approximately 6%, a pruned model achieves an accuracy of 75.36%, better than both unpruned versions. The largest residual architecture shown in Figure 8, i.e., ResNet-50, achieves an accuracy of 74.96% at a slightly larger complexity than the Inception-88 base.

Also, Figure 8 reveals that our grown series of deep Inception nets outperform the residual structures at similar complexities. As far as we know, this is the first time that a range of basic Inception structures are fairly compared against residual structures on the same input, at least in the complexity range we investigated. Another advantage of these deep Inception nets over the residual structures is that the former does not need to enforce the output dimensions of a module’s branches to be the same. Thus, it is of great potential to be used by other pruning approaches as well. Compared to the three fixed nets shown as five-pointed

stars in Fig. 8, the proposed pipeline not only achieves better accuracy at similar complexities but also offers a wide range of compact models for different accuracy and complexity requirements. From Fig. 8, we also notice that there is a sudden accuracy drop from ResNet-38 to ResNet-34. The former is the smallest ResNet consisting of depth-3 modules, while the latter (as defined in [19]) is the largest ResNet composed of depth-2 modules in our experiments.

5.3.2 Layerwise complexity

Figure 9 and 10 visualize layer-wise parameter and FLOPs complexity reduction results of our LDA pruning on the ‘grown-pushed’ Inception-88 model. From left to right, the conv layers within a Inception module are (1×1) , $(1 \times 1, 3 \times 3)$, $(1 \times 1, 3 \times 3a, 3 \times 3b)$, $(1 \times 1$ after pooling) layers.

According to Figure 9 and 10, most parameters and computations over the layers are pruned away, and different types of filters are pruned differently depending on the abstraction level and the scales where more task utility lies. As anticipated, the pruning rates of the first few layers, which capture commonly useful primitive patterns, are low. Almost all of the parameters and FLOPs are pruned away in

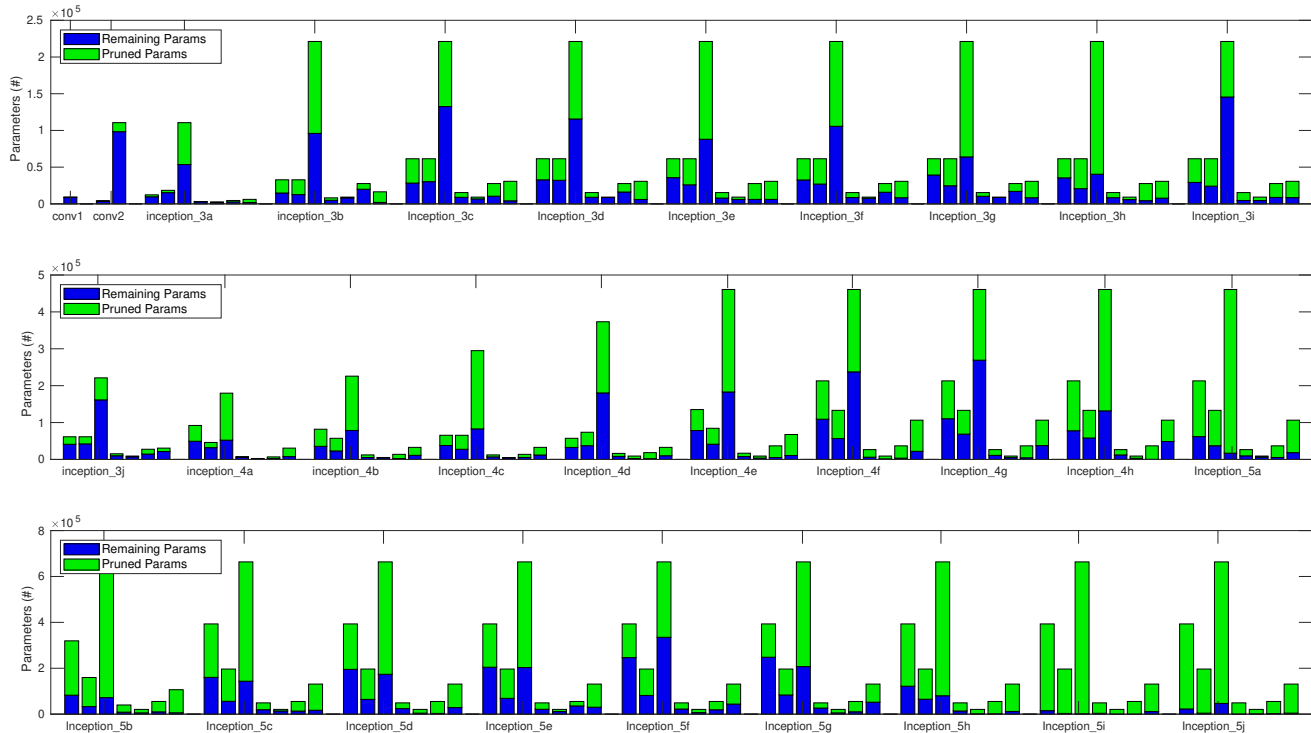


Figure 9: Layerwise parameter reductions of the grown Inception-88 on ImageNet. From left to right, the conv layers in a Inception module are (1×1) , $(1 \times 1, 3 \times 3)$, $(1 \times 1, 3 \times 3 a, 3 \times 3 b)$, $(1 \times 1$ after pooling). Green: pruned, blue: remaining. Due to the large network depth, the layer-wise parameter complexity figure is displayed in three rows. conv2 includes a dimension reducing layer in front (notation skipped because of space limit).

the last two modules, which can be regarded as an indicator that the depth is large enough (at least locally). This is in agreement with our observation at the growing step that adding one or two more modules to the Inception-88 net does not help much.

Interestingly, while the deep Inception net was greedily grown to achieve the highest accuracy locally, there are still massive redundant and useless structures over the layers. That is to say, at the growing step, each time we stacked one more module in the attempt to gain more accuracy, we simultaneously added more useless structures due to the ad hoc filter numbers used. Those useless structures cannot be effectively aligned with task utility even after training and can thus be discarded. The large pruning rates over the layers highlight the advantage of our deep LDA pruning over architecture hand-engineering with ad-hoc filter numbers.

6. Discussion and Future directions

Deep discriminant analysis (DDA), a non-linear generalization of LDA, is able to capture useful information embedded in the complex raw data space with the help of deeply learned transformation. Also, unlike LDA, DDA can possibly pick up high-order moments/statistics in the data.

In a concurrent work of ours, we are investigating our LDA pruning’s influence on model robustness. We believe that two important causes of adversarial vulnerability are over-fitting and the model’s inadequacy to accurately capture the task demands. Our conjecture is that adversarial attacks can trigger interfering features that are not aligned with task demands. The more such task-irrelevant features a model has, the higher the chance it will be hit by adversarial attacks and noises. By throwing away irrelevant structures, we are simultaneously mitigating overfitting and removing interfering parameters, thus possibly increasing the model robustness to irrelevant factors in the image space.

7. Conclusion

In this paper, instead of pruning based on an optimally pre-trained model, we have proposed a proactive approach following a two-step procedure in iterations. (1) through learning, it proactively unravels twisted threads of deep variation and pushes useful ones into easily-decoupled sub-structures. More specifically, it maximizes and decorrelates latent discriminants and pushes them into alignment with a subset of neurons. The deep LDA and covariance terms added are calculated per batch at the easily disen-

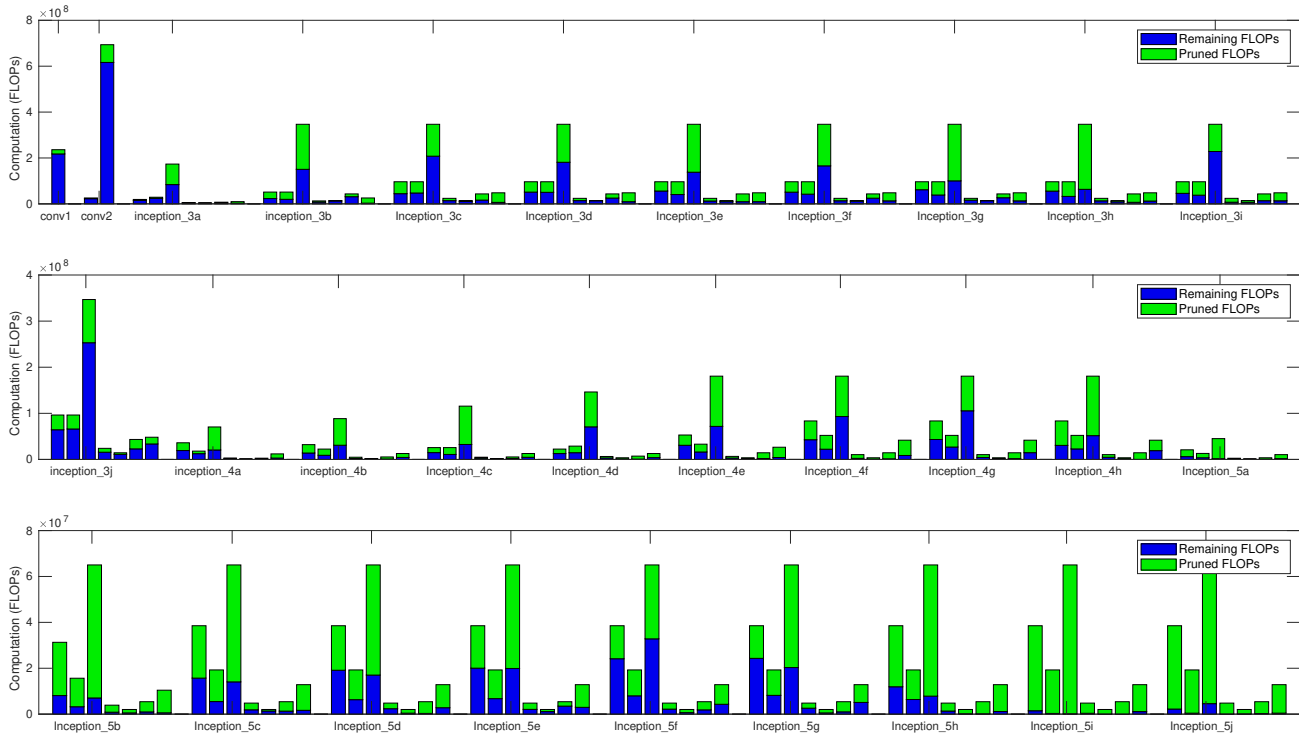


Figure 10: Layerwise FLOPs reductions of the grown Inception-88 on ImageNet. From left to right, the conv layers in a Inception module are (1×1) , $(1 \times 1, 3 \times 3)$, $(1 \times 1, 3 \times 3 \text{ a}, 3 \times 3 \text{ b})$, $(1 \times 1 \text{ after pooling})$. Green: pruned, blue: remaining. Due to the large network depth, the layer-wise FLOPs complexity figure is displayed in three rows. conv2 includes a dimension reducing layer in front (notation skipped because of space limit).

tangled top end, but exert influence over the layers. (2) After the essence is separated from the dregs, the second pruning step simply throws away the useless or even harmful dregs over the layers based on deconv tracing. Experiments on MNIST, CIFAR10, and ImageNet demonstrate the method’s efficacy.

Also, the starting base net is vital for compact network search. Its capacity should be large enough to encompass enough possible ‘winning lottery tickets’ while not too large to fit on available computing resources or to obviously overfit the data. In addition to adopting a fixed base, we explore to grow a base model. In the literature, ResNets have been one of the most popular and adopted architectures, mainly due to its ability to deal with complicated data with its very large depth. In contrast, most Inception nets achieve great expressive power with their wide variety of filter choices. By growing from the basic InceptionV1 net to an 88-layer-deep Inception variant, we show that Inception nets can actually be very deep while achieve better or at least comparable accuracy to ResNets at similar complexities. Most importantly, they have no hard-coded dimension agreement. Therefore, such architectures can provide more freedom for pruning methods. Also, the proposed growing

strategy based on basic Inception modules can potentially offer more plasticity for transfer learning and domain adaptation tasks.

By pushing and pruning on the grown network, we effectively combine bottom-up and top-down model search given a task. Experiments on ImageNet show that the combined compact architecture search pipeline is able to derive efficient models that achieve higher accuracy than the greedily-grown deep Inception nets, some residual architectures, and popular fixed nets at similar complexities.

References

- [1] Sajid Anwar, Kyuyeon Hwang, and Wonyong Sung. Structured pruning of deep convolutional neural networks. *arXiv preprint arXiv:1512.08571*, 2015. 2
- [2] Bowen Baker, Otakrist Gupta, Nikhil Naik, and Ramesh Raskar. Designing neural network architectures using reinforcement learning. *arXiv preprint arXiv:1611.02167*, 2016. 2
- [3] Yoshua Bengio, Grégoire Mesnil, Yann Dauphin, and Salah Rifai. Better mixing via deep representations. In *International conference on machine learning*, pages 552–560, 2013. 4

- [4] Andrew Brock, Theodore Lim, James M Ritchie, and Nick Weston. Smash: one-shot model architecture search through hypernetworks. *arXiv preprint arXiv:1708.05344*, 2017. 3
- [5] François Chollet. Xception: Deep learning with depthwise separable convolutions. In *Proceedings of the IEEE conference on computer vision and pattern recognition*, pages 1251–1258, 2017. 2
- [6] Matthieu Courbariaux, Yoshua Bengio, and Jean-Pierre David. Binaryconnect: Training deep neural networks with binary weights during propagations. In *Advances in neural information processing systems*, pages 3123–3131, 2015. 2
- [7] Emily L Denton, Wojciech Zaremba, Joan Bruna, Yann LeCun, and Rob Fergus. Exploiting linear structure within convolutional networks for efficient evaluation. In *Advances in neural information processing systems*, pages 1269–1277, 2014. 2
- [8] Ronen Eldan and Ohad Shamir. The power of depth for feed-forward neural networks. In *Conference on learning theory*, pages 907–940, 2016. 6
- [9] Ronald A Fisher. The use of multiple measurements in taxonomic problems. *Annals of eugenics*, 7(2):179–188, 1936. 4
- [10] Jonathan Frankle and Michael Carbin. The lottery ticket hypothesis: Finding sparse, trainable neural networks. 2019. 3, 6
- [11] Jerome H Friedman. Regularized discriminant analysis. *Journal of the American statistical association*, 84(405):165–175, 1989. 5
- [12] Yunchao Gong, Liu Liu, Ming Yang, and Lubomir Bourdev. Compressing deep convolutional networks using vector quantization. *arXiv preprint arXiv:1412.6115*, 2014. 2
- [13] Yiwen Guo, Anbang Yao, and Yurong Chen. Dynamic network surgery for efficient dnns. In *Advances In Neural Information Processing Systems*, pages 1379–1387, 2016. 2
- [14] Suyog Gupta, Ankur Agrawal, Kailash Gopalakrishnan, and Pritish Narayanan. Deep learning with limited numerical precision. In *International Conference on Machine Learning*, pages 1737–1746, 2015. 2
- [15] Song Han, Huizi Mao, and William J Dally. Deep compression: Compressing deep neural network with pruning, trained quantization and huffman coding. *CoRR, abs/1510.00149*, 2, 2015. 2
- [16] Song Han, Jeff Pool, John Tran, and William Dally. Learning both weights and connections for efficient neural network. In *Advances in Neural Information Processing Systems*, pages 1135–1143, 2015. 2, 9, 10
- [17] Babak Hassibi and David G Stork. *Second order derivatives for network pruning: Optimal brain surgeon*. Morgan Kaufmann, 1993. 2
- [18] Simon S Haykin. *Blind deconvolution*. Prentice Hall, 1994. 5
- [19] Kaiming He, Xiangyu Zhang, Shaoqing Ren, and Jian Sun. Deep residual learning for image recognition. *arXiv preprint arXiv:1512.03385*, 2015. 6, 10, 12, 13
- [20] Kaiming He, Xiangyu Zhang, Shaoqing Ren, and Jian Sun. Deep residual learning for image recognition. In *Proceedings of the IEEE conference on computer vision and pattern recognition*, pages 770–778, 2016. 2
- [21] Tong He, Zhi Zhang, Hang Zhang, Zhongyue Zhang, Junyuan Xie, and Mu Li. Bag of tricks for image classification with convolutional neural networks. In *Proceedings of the IEEE Conference on Computer Vision and Pattern Recognition*, pages 558–567, 2019. 8
- [22] Yihui He, Ji Lin, Zhijian Liu, Hanrui Wang, Li-Jia Li, and Song Han. Amc: Automl for model compression and acceleration on mobile devices. In *Proceedings of the European Conference on Computer Vision (ECCV)*, pages 784–800, 2018. 3
- [23] Yang He, Ping Liu, Ziwei Wang, Zhilan Hu, and Yi Yang. Filter pruning via geometric median for deep convolutional neural networks acceleration. In *Proceedings of the IEEE Conference on Computer Vision and Pattern Recognition*, pages 4340–4349, 2019. 2
- [24] Yihui He, Xiangyu Zhang, and Jian Sun. Channel pruning for accelerating very deep neural networks. In *Proceedings of the IEEE International Conference on Computer Vision*, pages 1389–1397, 2017. 2
- [25] Geoffrey Hinton, Oriol Vinyals, and Jeff Dean. Distilling the knowledge in a neural network. *arXiv preprint arXiv:1503.02531*, 2015. 2
- [26] Andrew G Howard, Menglong Zhu, Bo Chen, Dmitry Kalenichenko, Weijun Wang, Tobias Weyand, Marco Andreetto, and Hartwig Adam. Mobilenets: Efficient convolutional neural networks for mobile vision applications. *arXiv preprint arXiv:1704.04861*, 2017. 2, 10, 11, 12
- [27] Hengyuan Hu, Rui Peng, Yu-Wing Tai, and Chi-Keung Tang. Network trimming: A data-driven neuron pruning approach towards efficient deep architectures. *arXiv preprint arXiv:1607.03250*, 2016. 2
- [28] John D Hunter. Matplotlib: A 2d graphics environment. *Computing in science & engineering*, 9(3):90–95, 2007. 9
- [29] Forrest N Iandola, Song Han, Matthew W Moskewicz, Khalid Ashraf, William J Dally, and Kurt Keutzer. Squeezenet: Alexnet-level accuracy with 50x fewer parameters and <0.5 mb model size. *arXiv preprint arXiv:1602.07360*, 2016. 2, 10, 11, 12
- [30] Sergey Ioffe and Christian Szegedy. Batch normalization: Accelerating deep network training by reducing internal covariate shift. *arXiv preprint arXiv:1502.03167*, 2015. 7, 11, 12
- [31] Max Jaderberg, Andrea Vedaldi, and Andrew Zisserman. Speeding up convolutional neural networks with low rank expansions. *arXiv preprint arXiv:1405.3866*, 2014. 2
- [32] Xiaojie Jin, Xiaotong Yuan, Jiashi Feng, and Shuicheng Yan. Training skinny deep neural networks with iterative hard thresholding methods. *arXiv preprint arXiv:1607.05423*, 2016. 2
- [33] Alex Krizhevsky and Geoffrey Hinton. Learning multiple layers of features from tiny images. Technical report, 2009. 10
- [34] Yann LeCun, Léon Bottou, Yoshua Bengio, and Patrick Haffner. Gradient-based learning applied to document recognition. *Proceedings of the IEEE*, 86(11):2278–2324, 1998. 8

- [35] Yann LeCun, John S Denker, Sara A Solla, Richard E Howard, and Lawrence D Jackel. Optimal brain damage. In *NIPs*, volume 2, pages 598–605, 1989. 2
- [36] Hao Li, Asim Kadav, Igor Durdanovic, Hanan Samet, and Hans Peter Graf. Pruning filters for efficient convnets. *arXiv preprint arXiv:1608.08710*, 2016. 2
- [37] Chenxi Liu, Barret Zoph, Maxim Neumann, Jonathon Shlens, Wei Hua, Li-Jia Li, Li Fei-Fei, Alan Yuille, Jonathan Huang, and Kevin Murphy. Progressive neural architecture search. In *Proceedings of the European Conference on Computer Vision (ECCV)*, pages 19–34, 2018. 3
- [38] Zelda Mariet and Suvrit Sra. Diversity networks. 2016. 2
- [39] Hrushikesh Mhaskar, Qianli Liao, and Tomaso Poggio. Learning functions: when is deep better than shallow. *arXiv preprint arXiv:1603.00988*, 2016. 6
- [40] Risto Miikkulainen, Jason Liang, Elliot Meyerson, Aditya Rawal, Dan Fink, Olivier Francon, Bala Raju, Arshak Navruzyan, Nigel Duffy, and Babak Hodjat. Evolving deep neural networks. *arXiv preprint arXiv:1703.00548*, 2017. 2
- [41] Pavlo Molchanov, Arun Mallya, Stephen Tyree, Iuri Frosio, and Jan Kautz. Importance estimation for neural network pruning. In *Proceedings of the IEEE Conference on Computer Vision and Pattern Recognition*, pages 11264–11272, 2019. 2
- [42] Pavlo Molchanov, Stephen Tyree, Tero Karras, Timo Aila, and Jan Kautz. Pruning convolutional neural networks for resource efficient inference. *arXiv preprint arXiv:1611.06440*, 2016. 10, 11
- [43] Renato Negrinho and Geoff Gordon. Deeparchitect: Automatically designing and training deep architectures. *arXiv preprint arXiv:1704.08792*, 2017. 3
- [44] Hieu Pham, Melody Y Guan, Barret Zoph, Quoc V Le, and Jeff Dean. Efficient neural architecture search via parameter sharing. *arXiv preprint arXiv:1802.03268*, 2018. 3
- [45] Tomaso Poggio, Hrushikesh Mhaskar, Lorenzo Rosasco, Brando Miranda, and Qianli Liao. Why and when can deep-but not shallow-networks avoid the curse of dimensionality: a review. *International Journal of Automation and Computing*, 14(5):503–519, 2017. 6
- [46] Adam Polyak and Lior Wolf. Channel-level acceleration of deep face representations. *IEEE Access*, 3:2163–2175, 2015. 2
- [47] Lorien Y Pratt. *Comparing biases for minimal network construction with back-propagation*, volume 1. Morgan Kaufmann Pub, 1989. 2
- [48] C Radhakrishna Rao. The utilization of multiple measurements in problems of biological classification. *Journal of the Royal Statistical Society. Series B (Methodological)*, 10(2):159–203, 1948. 4
- [49] Mohammad Rastegari, Vicente Ordonez, Joseph Redmon, and Ali Farhadi. Xnor-net: Imagenet classification using binary convolutional neural networks. In *European Conference on Computer Vision*, pages 525–542. Springer, 2016. 2
- [50] Esteban Real, Alok Aggarwal, Yanping Huang, and Quoc V Le. Regularized evolution for image classifier architecture search. *arXiv preprint arXiv:1802.01548*, 2018. 2, 3
- [51] Esteban Real, Sherry Moore, Andrew Selle, Saurabh Saxena, Yutaka Leon Suematsu, Quoc Le, and Alex Kurakin. Large-scale evolution of image classifiers. *arXiv preprint arXiv:1703.01041*, 2017. 2, 3
- [52] Russell Reed. Pruning algorithms—a survey. *IEEE transactions on Neural Networks*, 4(5):740–747, 1993. 2
- [53] Itay Safran and Ohad Shamir. Depth-width tradeoffs in approximating natural functions with neural networks. In *Proceedings of the 34th International Conference on Machine Learning—Volume 70*, pages 2979–2987. JMLR. org, 2017. 6
- [54] Suraj Srinivas and R Venkatesh Babu. Data-free parameter pruning for deep neural networks. *arXiv preprint arXiv:1507.06149*, 2015. 2
- [55] Kenneth O Stanley and Risto Miikkulainen. Evolving neural networks through augmenting topologies. *Evolutionary computation*, 10(2):99–127, 2002. 2
- [56] Fangxuan Sun and Jun Lin. Memory efficient nonuniform quantization for deep convolutional neural network. *arXiv preprint arXiv, 1607*, 2016. 2
- [57] Vivienne Sze, Tien-Ju Yang, and Yu-Hsin Chen. Designing energy-efficient convolutional neural networks using energy-aware pruning. pages 5687–5695, 2017. 2
- [58] Christian Szegedy, Wei Liu, Yangqing Jia, Pierre Sermanet, Scott Reed, Dragomir Anguelov, Dumitru Erhan, Vincent Vanhoucke, and Andrew Rabinovich. Going deeper with convolutions. In *Proceedings of the IEEE Conference on Computer Vision and Pattern Recognition*, pages 1–9, 2015. 2, 6
- [59] Matus Telgarsky. Benefits of depth in neural networks. In *Conference on Learning Theory*, pages 1517–1539, 2016. 6
- [60] Qing Tian, Tal Arbel, and James J Clark. Deep l1-pruned nets for efficient facial gender classification. In *Computer Vision and Pattern Recognition Workshops (CVPR Workshop on Biometrics)*, 2017 *IEEE Conference on*, pages 512–521. IEEE, 2017. 2, 3
- [61] Qing Tian, Tal Arbel, and James J Clark. Structured deep fisher pruning for efficient facial trait classification. *Image and Vision Computing*, 77:45–59, 2018. 2
- [62] Qing Tian, Tal Arbel, and James J Clark. Task-specific deep l1 pruning of neural networks. *arXiv preprint arXiv:1803.08134*, 2018. 5, 10, 11
- [63] Lingxi Xie and Alan Yuille. Genetic cnn. *arXiv preprint arXiv:1703.01513*, 2017. 2
- [64] Matthew D Zeiler and Rob Fergus. Visualizing and understanding convolutional networks. In *European Conference on Computer Vision*, pages 818–833. Springer, 2014. 4, 5
- [65] Xiangyu Zhang, Jianhua Zou, Kaiming He, and Jian Sun. Accelerating very deep convolutional networks for classification and detection. *IEEE transactions on pattern analysis and machine intelligence*, 38(10):1943–1955, 2016. 2
- [66] Zhao Zhong, Junjie Yan, Wei Wu, Jing Shao, and Cheng-Lin Liu. Practical block-wise neural network architecture generation. *arXiv preprint arXiv:1708.05552*, 2017. 2
- [67] Zhuangwei Zhuang, Minghui Tan, Bohan Zhuang, Jing Liu, Yong Guo, Qingyao Wu, Junzhou Huang, and Jinhui Zhu. Discrimination-aware channel pruning for deep neural networks. In *Advances in Neural Information Processing Systems*, pages 875–886, 2018. 2

- [68] Barret Zoph and Quoc V Le. Neural architecture search with reinforcement learning. *arXiv preprint arXiv:1611.01578*, 2016. [2](#), [3](#)
- [69] Barret Zoph, Vijay Vasudevan, Jonathon Shlens, and Quoc V Le. Learning transferable architectures for scalable image recognition. *arXiv preprint arXiv:1707.07012*, 2017. [2](#)

A. Appendix - Inception-88 Architecture

```
def create_deepinception88(weights_path=None):

    concat_axis = 1 if K.image_data_format() == 'channels_first' else -1

    img_input = Input(shape=(224, 224, 3))
    if K.image_data_format() == 'channels_first':
        x = Lambda(lambda x: K.permute_dimensions(x, (0, 3, 1, 2)), name='transpose')(img_input)
    else: # channels_last
        x = img_input

    # manual padding and valid mode for framework compatibility
    x_pad = ZeroPadding2D(padding=(3, 3))(x)
    conv1_7x7_s2 = Conv2D_bn(x_pad, 64, (7, 7), strides=(2, 2), padding='valid', name='conv1/7x7_s2')

    #####
    # Pooling
    #####
    pool1_3x3_s2 = MaxPooling2D(pool_size=(3, 3), strides=(2, 2), padding='same', name='pool1/3x3_s2')(conv1_7x7_s2)

    conv2_3x3_reduce = Conv2D_bn(pool1_3x3_s2, 64, (1, 1), name='conv2/3x3_reduce')

    conv2_3x3 = Conv2D_bn(conv2_3x3_reduce, 192, (3, 3), name='conv2/3x3')

    #####
    # Pooling
    #####
    pool2_3x3_s2 = MaxPooling2D(pool_size=(3, 3), strides=(2, 2), padding='same', name='pool2/3x3_s2')(conv2_3x3)

    #####
    inception_3a_1x1 = Conv2D_bn(pool2_3x3_s2, 64, (1, 1), name='inception_3a/1x1')

    inception_3a_3x3_reduce = Conv2D_bn(pool2_3x3_s2, 96, (1, 1), name='inception_3a/3x3_reduce')
    inception_3a_3x3 = Conv2D_bn(inception_3a_3x3_reduce, 128, (3, 3), name='inception_3a/3x3')

    inception_3a_5x5_reduce = Conv2D_bn(pool2_3x3_s2, 16, (1, 1), name='inception_3a/5x5_reduce')
    inception_3a_double3x3a = Conv2D_bn(inception_3a_5x5_reduce, 16, (3, 3), name='inception_3a/double3x3a')
    inception_3a_double3x3b = Conv2D_bn(inception_3a_double3x3a, 32, (3, 3), name='inception_3a/double3x3b')

    inception_3a_pool = AveragePooling2D(pool_size=(3, 3), strides=(1, 1), padding='same', name='inception_3a/pool')(pool2_3x3_s2)
    inception_3a_pool_proj = Conv2D_bn(inception_3a_pool, 32, (1, 1), name='inception_3a/pool_proj')

    inception_3a_output = concatenate([inception_3a_1x1, inception_3a_3x3, inception_3a_double3x3b, inception_3a_pool_proj], axis=concat_axis, name='inception_3a/output')

    #####
    inception_3b_1x1 = Conv2D_bn(inception_3a_output, 128, (1, 1), name='inception_3b/1x1')

    inception_3b_3x3_reduce = Conv2D_bn(inception_3a_output, 128, (1, 1), name='inception_3b/3x3_reduce')
    inception_3b_3x3 = Conv2D_bn(inception_3b_3x3_reduce, 192, (3, 3), name='inception_3b/3x3')

    inception_3b_5x5_reduce = Conv2D_bn(inception_3a_output, 32, (1, 1), name='inception_3b/5x5_reduce')
    inception_3b_double3x3a = Conv2D_bn(inception_3b_5x5_reduce, 32, (3, 3), name='inception_3b/double3x3a')
    inception_3b_double3x3b = Conv2D_bn(inception_3b_double3x3a, 96, (3, 3), name='inception_3b/double3x3b')

    inception_3b_pool = AveragePooling2D(pool_size=(3, 3), strides=(1, 1), padding='same', name='inception_3b/pool')(inception_3a_output)
    inception_3b_pool_proj = Conv2D_bn(inception_3b_pool, 64, (1, 1), name='inception_3b/pool_proj')

    inception_3b_output = concatenate([inception_3b_1x1, inception_3b_3x3, inception_3b_double3x3b, inception_3b_pool_proj], axis=concat_axis, name='inception_3b/output')

    #####
    inception_3c_1x1 = Conv2D_bn(inception_3b_output, 128, (1, 1), name='inception_3c/1x1')

    inception_3c_3x3_reduce = Conv2D_bn(inception_3b_output, 128, (1, 1), name='inception_3c/3x3_reduce')
    inception_3c_3x3 = Conv2D_bn(inception_3c_3x3_reduce, 192, (3, 3), name='inception_3c/3x3')

    inception_3c_5x5_reduce = Conv2D_bn(inception_3b_output, 32, (1, 1), name='inception_3c/5x5_reduce')
    inception_3c_double3x3a = Conv2D_bn(inception_3c_5x5_reduce, 32, (3, 3), name='inception_3c/double3x3a')
    inception_3c_double3x3b = Conv2D_bn(inception_3c_double3x3a, 96, (3, 3), name='inception_3c/double3x3b')

    inception_3c_pool = AveragePooling2D(pool_size=(3, 3), strides=(1, 1), padding='same', name='inception_3c/pool')(inception_3b_output)
    inception_3c_pool_proj = Conv2D_bn(inception_3c_pool, 64, (1, 1), name='inception_3c/pool_proj')

    inception_3c_output = concatenate([inception_3c_1x1, inception_3c_3x3, inception_3c_double3x3b, inception_3c_pool_proj], axis=concat_axis, name='inception_3c/output')

    #####
    inception_3d_1x1 = Conv2D_bn(inception_3c_output, 128, (1, 1), name='inception_3d/1x1')

    inception_3d_3x3_reduce = Conv2D_bn(inception_3c_output, 128, (1, 1), name='inception_3d/3x3_reduce')
    inception_3d_3x3 = Conv2D_bn(inception_3d_3x3_reduce, 192, (3, 3), name='inception_3d/3x3')

    inception_3d_5x5_reduce = Conv2D_bn(inception_3c_output, 32, (1, 1), name='inception_3d/5x5_reduce')
    inception_3d_double3x3a = Conv2D_bn(inception_3d_5x5_reduce, 32, (3, 3), name='inception_3d/double3x3a')
    inception_3d_double3x3b = Conv2D_bn(inception_3d_double3x3a, 96, (3, 3), name='inception_3d/double3x3b')

    inception_3d_pool = AveragePooling2D(pool_size=(3, 3), strides=(1, 1), padding='same', name='inception_3d/pool')(inception_3c_output)
    inception_3d_pool_proj = Conv2D_bn(inception_3d_pool, 64, (1, 1), name='inception_3d/pool_proj')

    inception_3d_output = concatenate([inception_3d_1x1, inception_3d_3x3, inception_3d_double3x3b, inception_3d_pool_proj], axis=concat_axis, name='inception_3d/output')

    #####
    inception_3e_1x1 = Conv2D_bn(inception_3d_output, 128, (1, 1), name='inception_3e/1x1')

    inception_3e_3x3_reduce = Conv2D_bn(inception_3d_output, 128, (1, 1), name='inception_3e/3x3_reduce')
    inception_3e_3x3 = Conv2D_bn(inception_3e_3x3_reduce, 192, (3, 3), name='inception_3e/3x3')

    inception_3e_5x5_reduce = Conv2D_bn(inception_3d_output, 32, (1, 1), name='inception_3e/5x5_reduce')
    inception_3e_double3x3a = Conv2D_bn(inception_3e_5x5_reduce, 32, (3, 3), name='inception_3e/double3x3a')
    inception_3e_double3x3b = Conv2D_bn(inception_3e_double3x3a, 96, (3, 3), name='inception_3e/double3x3b')
```

```
inception_3e_pool = AveragePooling2D(pool_size=(3,3), strides=(1,1), padding='same', name='inception_3e/pool')(inception_3d_output)
inception_3e_pool_proj = Conv2D_bn(inception_3e_pool, 64, (1,1), name='inception_3e/pool_proj')

inception_3e_output = concatenate([inception_3e_1x1, inception_3e_3x3, inception_3e_double3x3b, inception_3e_pool_proj], axis=concat_axis, name='inception_3e/output')
#####

inception_3f_1x1 = Conv2D_bn(inception_3e_output, 128, (1,1), name='inception_3f/1x1')

inception_3f_3x3_reduce = Conv2D_bn(inception_3e_output, 128, (1,1), name='inception_3f/3x3_reduce')
inception_3f_3x3 = Conv2D_bn(inception_3f_3x3_reduce, 192, (3,3), name='inception_3f/3x3')

inception_3f_5x5_reduce = Conv2D_bn(inception_3e_output, 32, (1,1), name='inception_3f/5x5_reduce')
inception_3f_double3x3a = Conv2D_bn(inception_3f_5x5_reduce, 32, (3,3), name='inception_3f/double3x3a')
inception_3f_double3x3b = Conv2D_bn(inception_3f_double3x3a, 96, (3,3), name='inception_3f/double3x3b')

inception_3f_pool = AveragePooling2D(pool_size=(3,3), strides=(1,1), padding='same', name='inception_3f/pool')(inception_3e_output)
inception_3f_pool_proj = Conv2D_bn(inception_3f_pool, 64, (1,1), name='inception_3f/pool_proj')

inception_3f_output = concatenate([inception_3f_1x1, inception_3f_3x3, inception_3f_double3x3b, inception_3f_pool_proj], axis=concat_axis, name='inception_3f/output')
#####

inception_3g_1x1 = Conv2D_bn(inception_3f_output, 128, (1,1), name='inception_3g/1x1')

inception_3g_3x3_reduce = Conv2D_bn(inception_3f_output, 128, (1,1), name='inception_3g/3x3_reduce')
inception_3g_3x3 = Conv2D_bn(inception_3g_3x3_reduce, 192, (3,3), name='inception_3g/3x3')

inception_3g_5x5_reduce = Conv2D_bn(inception_3f_output, 32, (1,1), name='inception_3g/5x5_reduce')
inception_3g_double3x3a = Conv2D_bn(inception_3g_5x5_reduce, 32, (3,3), name='inception_3g/double3x3a')
inception_3g_double3x3b = Conv2D_bn(inception_3g_double3x3a, 96, (3,3), name='inception_3g/double3x3b')

inception_3g_pool = AveragePooling2D(pool_size=(3,3), strides=(1,1), padding='same', name='inception_3g/pool')(inception_3f_output)
inception_3g_pool_proj = Conv2D_bn(inception_3g_pool, 64, (1,1), name='inception_3g/pool_proj')

inception_3g_output = concatenate([inception_3g_1x1, inception_3g_3x3, inception_3g_double3x3b, inception_3g_pool_proj], axis=concat_axis, name='inception_3g/output')
#####

inception_3h_1x1 = Conv2D_bn(inception_3g_output, 128, (1,1), name='inception_3h/1x1')

inception_3h_3x3_reduce = Conv2D_bn(inception_3g_output, 128, (1,1), name='inception_3h/3x3_reduce')
inception_3h_3x3 = Conv2D_bn(inception_3h_3x3_reduce, 192, (3,3), name='inception_3h/3x3')

inception_3h_5x5_reduce = Conv2D_bn(inception_3g_output, 32, (1,1), name='inception_3h/5x5_reduce')
inception_3h_double3x3a = Conv2D_bn(inception_3h_5x5_reduce, 32, (3,3), name='inception_3h/double3x3a')
inception_3h_double3x3b = Conv2D_bn(inception_3h_double3x3a, 96, (3,3), name='inception_3h/double3x3b')

inception_3h_pool = AveragePooling2D(pool_size=(3,3), strides=(1,1), padding='same', name='inception_3h/pool')(inception_3g_output)
inception_3h_pool_proj = Conv2D_bn(inception_3h_pool, 64, (1,1), name='inception_3h/pool_proj')

inception_3h_output = concatenate([inception_3h_1x1, inception_3h_3x3, inception_3h_double3x3b, inception_3h_pool_proj], axis=concat_axis, name='inception_3h/output')
#####

inception_3i_1x1 = Conv2D_bn(inception_3h_output, 128, (1,1), name='inception_3i/1x1')

inception_3i_3x3_reduce = Conv2D_bn(inception_3h_output, 128, (1,1), name='inception_3i/3x3_reduce')
inception_3i_3x3 = Conv2D_bn(inception_3i_3x3_reduce, 192, (3,3), name='inception_3i/3x3')

inception_3i_5x5_reduce = Conv2D_bn(inception_3h_output, 32, (1,1), name='inception_3i/5x5_reduce')
inception_3i_double3x3a = Conv2D_bn(inception_3i_5x5_reduce, 32, (3,3), name='inception_3i/double3x3a')
inception_3i_double3x3b = Conv2D_bn(inception_3i_double3x3a, 96, (3,3), name='inception_3i/double3x3b')

inception_3i_pool = AveragePooling2D(pool_size=(3,3), strides=(1,1), padding='same', name='inception_3i/pool')(inception_3h_output)
inception_3i_pool_proj = Conv2D_bn(inception_3i_pool, 64, (1,1), name='inception_3i/pool_proj')

inception_3i_output = concatenate([inception_3i_1x1, inception_3i_3x3, inception_3i_double3x3b, inception_3i_pool_proj], axis=concat_axis, name='inception_3i/output')
#####

inception_3j_1x1 = Conv2D_bn(inception_3i_output, 128, (1,1), name='inception_3j/1x1')

inception_3j_3x3_reduce = Conv2D_bn(inception_3i_output, 128, (1,1), name='inception_3j/3x3_reduce')
inception_3j_3x3 = Conv2D_bn(inception_3j_3x3_reduce, 192, (3,3), name='inception_3j/3x3')

inception_3j_5x5_reduce = Conv2D_bn(inception_3i_output, 32, (1,1), name='inception_3j/5x5_reduce')
inception_3j_double3x3a = Conv2D_bn(inception_3j_5x5_reduce, 32, (3,3), name='inception_3j/double3x3a')
inception_3j_double3x3b = Conv2D_bn(inception_3j_double3x3a, 96, (3,3), name='inception_3j/double3x3b')

inception_3j_pool = AveragePooling2D(pool_size=(3,3), strides=(1,1), padding='same', name='inception_3j/pool')(inception_3i_output)
inception_3j_pool_proj = Conv2D_bn(inception_3j_pool, 64, (1,1), name='inception_3j/pool_proj')

inception_3j_output = concatenate([inception_3j_1x1, inception_3j_3x3, inception_3j_double3x3b, inception_3j_pool_proj], axis=concat_axis, name='inception_3j/output')
#####
# Pooling
#####
pool3_3x3_s2 = MaxPooling2D(pool_size=(3,3), strides=(2,2), padding='same', name='pool3/3x3_s2')(inception_3j_output)
#####

inception_4a_1x1 = Conv2D_bn(pool3_3x3_s2, 192, (1,1), name='inception_4a/1x1')

inception_4a_3x3_reduce = Conv2D_bn(pool3_3x3_s2, 96, (1,1), name='inception_4a/3x3_reduce')
inception_4a_3x3 = Conv2D_bn(inception_4a_3x3_reduce, 208, (3,3), name='inception_4a/3x3')

inception_4a_5x5_reduce = Conv2D_bn(pool3_3x3_s2, 16, (1,1), name='inception_4a/5x5_reduce')
inception_4a_double3x3a = Conv2D_bn(inception_4a_5x5_reduce, 16, (3,3), name='inception_4a/double3x3a')
inception_4a_double3x3b = Conv2D_bn(inception_4a_double3x3a, 48, (3,3), name='inception_4a/double3x3b')

inception_4a_pool = AveragePooling2D(pool_size=(3,3), strides=(1,1), padding='same', name='inception_4a/pool')(pool3_3x3_s2)
inception_4a_pool_proj = Conv2D_bn(inception_4a_pool, 64, (1,1), name='inception_4a/pool_proj')

inception_4a_output = concatenate([inception_4a_1x1, inception_4a_3x3, inception_4a_double3x3b, inception_4a_pool_proj], axis=concat_axis, name='inception_4a/output')
)
```

#####

```
loss1_ave_pool = AveragePooling2D(pool_size=(5,5), strides=(3,3), name='loss1/ave_pool')(inception_4a_output)
loss1_conv = Conv2D_bn(loss1_ave_pool, 128, (1,1), name='loss1/conv')
loss1_flat = Flatten()(loss1_conv)
loss1_fc = Dense(1024, activation='relu', name='loss1/fc', kernel_regularizer=l2(L2_WEIGHT_DECAY))(loss1_flat)
loss1_classifier = Dense(1000, name='loss1/classifier', kernel_regularizer=l2(L2_WEIGHT_DECAY))(loss1_fc)
loss1_classifier_act = Activation('softmax')(loss1_classifier)
```

#####

```
inception_4b_1x1 = Conv2D_bn(inception_4a_output, 160, (1,1), name='inception_4b/1x1')

inception_4b_3x3_reduce = Conv2D_bn(inception_4a_output, 112, (1,1), name='inception_4b/3x3_reduce')
inception_4b_3x3 = Conv2D_bn(inception_4b_3x3_reduce, 224, (3,3), name='inception_4b/3x3')

inception_4b_5x5_reduce = Conv2D_bn(inception_4a_output, 24, (1,1), name='inception_4b/5x5_reduce')
inception_4b_double3x3a = Conv2D_bn(inception_4b_5x5_reduce, 24, (3,3), name='inception_4b/double3x3a')
inception_4b_double3x3b = Conv2D_bn(inception_4b_double3x3a, 64, (3,3), name='inception_4b/double3x3b')

inception_4b_pool = AveragePooling2D(pool_size=(3,3), strides=(1,1), padding='same', name='inception_4b/pool')(inception_4a_output)
inception_4b_pool_proj = Conv2D_bn(inception_4b_pool, 64, (1,1), name='inception_4b/pool_proj')

inception_4b_output = concatenate([inception_4b_1x1, inception_4b_3x3, inception_4b_double3x3b, inception_4b_pool_proj], axis=concat_axis, name='inception_4b_output')
```

#####

```
inception_4c_1x1 = Conv2D_bn(inception_4b_output, 128, (1,1), name='inception_4c/1x1')

inception_4c_3x3_reduce = Conv2D_bn(inception_4b_output, 128, (1,1), name='inception_4c/3x3_reduce')
inception_4c_3x3 = Conv2D_bn(inception_4c_3x3_reduce, 256, (3,3), name='inception_4c/3x3')

inception_4c_5x5_reduce = Conv2D_bn(inception_4b_output, 24, (1,1), name='inception_4c/5x5_reduce')
inception_4c_double3x3a = Conv2D_bn(inception_4c_5x5_reduce, 24, (3,3), name='inception_4c/double3x3a')
inception_4c_double3x3b = Conv2D_bn(inception_4c_double3x3a, 64, (3,3), name='inception_4c/double3x3b')

inception_4c_pool = AveragePooling2D(pool_size=(3,3), strides=(1,1), padding='same', name='inception_4c/pool')(inception_4b_output)
inception_4c_pool_proj = Conv2D_bn(inception_4c_pool, 64, (1,1), name='inception_4c/pool_proj')

inception_4c_output = concatenate([inception_4c_1x1, inception_4c_3x3, inception_4c_double3x3b, inception_4c_pool_proj], axis=concat_axis, name='inception_4c/output')
```

#####

```
inception_4d_1x1 = Conv2D_bn(inception_4c_output, 112, (1,1), name='inception_4d/1x1')

inception_4d_3x3_reduce = Conv2D_bn(inception_4c_output, 144, (1,1), name='inception_4d/3x3_reduce')
inception_4d_3x3 = Conv2D_bn(inception_4d_3x3_reduce, 288, (3,3), name='inception_4d/3x3')

inception_4d_5x5_reduce = Conv2D_bn(inception_4c_output, 32, (1,1), name='inception_4d/5x5_reduce')
inception_4d_double3x3a = Conv2D_bn(inception_4d_5x5_reduce, 32, (3,3), name='inception_4d/double3x3a')
inception_4d_double3x3b = Conv2D_bn(inception_4d_double3x3a, 64, (3,3), name='inception_4d/double3x3b')

inception_4d_pool = AveragePooling2D(pool_size=(3,3), strides=(1,1), padding='same', name='inception_4d/pool')(inception_4c_output)
inception_4d_pool_proj = Conv2D_bn(inception_4d_pool, 64, (1,1), name='inception_4d/pool_proj')

inception_4d_output = concatenate([inception_4d_1x1, inception_4d_3x3, inception_4d_double3x3b, inception_4d_pool_proj], axis=concat_axis, name='inception_4d/output')
```

#####

```
inception_4e_1x1 = Conv2D_bn(inception_4d_output, 256, (1,1), name='inception_4e/1x1')

inception_4e_3x3_reduce = Conv2D_bn(inception_4d_output, 160, (1,1), name='inception_4e/3x3_reduce')
inception_4e_3x3 = Conv2D_bn(inception_4e_3x3_reduce, 320, (3,3), name='inception_4e/3x3')

inception_4e_5x5_reduce = Conv2D_bn(inception_4d_output, 32, (1,1), name='inception_4e/5x5_reduce')
inception_4e_double3x3a = Conv2D_bn(inception_4e_5x5_reduce, 32, (3,3), name='inception_4e/double3x3a')
inception_4e_double3x3b = Conv2D_bn(inception_4e_double3x3a, 128, (3,3), name='inception_4e/double3x3b')

inception_4e_pool = AveragePooling2D(pool_size=(3,3), strides=(1,1), padding='same', name='inception_4e/pool')(inception_4d_output)
inception_4e_pool_proj = Conv2D_bn(inception_4e_pool, 128, (1,1), name='inception_4e/pool_proj')

inception_4e_output = concatenate([inception_4e_1x1, inception_4e_3x3, inception_4e_double3x3b, inception_4e_pool_proj], axis=concat_axis, name='inception_4e/output')
```

#####

```
inception_4f_1x1 = Conv2D_bn(inception_4e_output, 256, (1,1), name='inception_4f/1x1')

inception_4f_3x3_reduce = Conv2D_bn(inception_4e_output, 160, (1,1), name='inception_4f/3x3_reduce')
inception_4f_3x3 = Conv2D_bn(inception_4f_3x3_reduce, 320, (3,3), name='inception_4f/3x3')

inception_4f_5x5_reduce = Conv2D_bn(inception_4e_output, 32, (1,1), name='inception_4f/5x5_reduce')
inception_4f_double3x3a = Conv2D_bn(inception_4f_5x5_reduce, 32, (3,3), name='inception_4f/double3x3a')
inception_4f_double3x3b = Conv2D_bn(inception_4f_double3x3a, 128, (3,3), name='inception_4f/double3x3b')

inception_4f_pool = AveragePooling2D(pool_size=(3,3), strides=(1,1), padding='same', name='inception_4f/pool')(inception_4e_output)
inception_4f_pool_proj = Conv2D_bn(inception_4f_pool, 128, (1,1), name='inception_4f/pool_proj')

inception_4f_output = concatenate([inception_4f_1x1, inception_4f_3x3, inception_4f_double3x3b, inception_4f_pool_proj], axis=concat_axis, name='inception_4f/output')
```

#####

```
inception_4g_1x1 = Conv2D_bn(inception_4f_output, 256, (1,1), name='inception_4g/1x1')

inception_4g_3x3_reduce = Conv2D_bn(inception_4f_output, 160, (1,1), name='inception_4g/3x3_reduce')
inception_4g_3x3 = Conv2D_bn(inception_4g_3x3_reduce, 320, (3,3), name='inception_4g/3x3')

inception_4g_5x5_reduce = Conv2D_bn(inception_4f_output, 32, (1,1), name='inception_4g/5x5_reduce')
inception_4g_double3x3a = Conv2D_bn(inception_4g_5x5_reduce, 32, (3,3), name='inception_4g/double3x3a')
inception_4g_double3x3b = Conv2D_bn(inception_4g_double3x3a, 128, (3,3), name='inception_4g/double3x3b')

inception_4g_pool = AveragePooling2D(pool_size=(3,3), strides=(1,1), padding='same', name='inception_4g/pool')(inception_4f_output)
inception_4g_pool_proj = Conv2D_bn(inception_4g_pool, 128, (1,1), name='inception_4g/pool_proj')

inception_4g_output = concatenate([inception_4g_1x1, inception_4g_3x3, inception_4g_double3x3b, inception_4g_pool_proj], axis=concat_axis, name='inception_4g/output')
```

```
#####
loss2_ave_pool = AveragePooling2D(pool_size=(5,5), strides=(3,3), name='loss2/ave_pool')(inception_4g_output)
loss2_conv = Conv2D_bn(loss2_ave_pool, 128, (1,1), name='loss2/conv')
loss2_flat = Flatten()(loss2_conv)
loss2_fc = Dense(1024, activation='relu', name='loss2/fc', kernel_regularizer=L2_WEIGHT_DECAY)(loss2_flat)
loss2_classifier = Dense(1000, name='loss2/classifier', kernel_regularizer=L2_WEIGHT_DECAY)(loss2_fc)
loss2_classifier_act = Activation('softmax')(loss2_classifier)

#####
inception_4h_1x1 = Conv2D_bn(inception_4g_output, 256, (1,1), name='inception_4h/1x1')

inception_4h_3x3_reduce = Conv2D_bn(inception_4g_output, 160, (1,1), name='inception_4h/3x3_reduce')
inception_4h_3x3 = Conv2D_bn(inception_4h_3x3_reduce, 320, (3,3), name='inception_4h/3x3')

inception_4h_5x5_reduce = Conv2D_bn(inception_4g_output, 32, (1,1), name='inception_4h/5x5_reduce')
inception_4h_double3x3a = Conv2D_bn(inception_4h_5x5_reduce, 32, (3,3), name='inception_4h/double3x3a')
inception_4h_double3x3b = Conv2D_bn(inception_4h_double3x3a, 128, (3,3), name='inception_4h/double3x3b')

inception_4h_pool = AveragePooling2D(pool_size=(3,3), strides=(1,1), padding='same', name='inception_4h/pool')(inception_4g_output)
inception_4h_pool_proj = Conv2D_bn(inception_4h_pool, 128, (1,1), name='inception_4h/pool_proj')

inception_4h_output = concatenate([inception_4h_1x1, inception_4h_3x3, inception_4h_double3x3b, inception_4h_pool_proj], axis=concat_axis, name='inception_4h/output')

#####
# Pooling
#####
pool4_3x3_s2 = MaxPooling2D(pool_size=(3,3), strides=(2,2), padding='same', name='pool4/3x3_s2')(inception_4h_output)

#####
inception_5a_1x1 = Conv2D_bn(pool4_3x3_s2, 256, (1,1), name='inception_5a/1x1')

inception_5a_3x3_reduce = Conv2D_bn(pool4_3x3_s2, 160, (1,1), name='inception_5a/3x3_reduce')
inception_5a_3x3 = Conv2D_bn(inception_5a_3x3_reduce, 320, (3,3), name='inception_5a/3x3')

inception_5a_5x5_reduce = Conv2D_bn(pool4_3x3_s2, 32, (1,1), name='inception_5a/5x5_reduce')
inception_5a_double3x3a = Conv2D_bn(inception_5a_5x5_reduce, 32, (3,3), name='inception_5a/double3x3a')
inception_5a_double3x3b = Conv2D_bn(inception_5a_double3x3a, 128, (3,3), name='inception_5a/double3x3b')

inception_5a_pool = AveragePooling2D(pool_size=(3,3), strides=(1,1), padding='same', name='inception_5a/pool')(pool4_3x3_s2)
inception_5a_pool_proj = Conv2D_bn(inception_5a_pool, 128, (1,1), name='inception_5a/pool_proj')

inception_5a_output = concatenate([inception_5a_1x1, inception_5a_3x3, inception_5a_double3x3b, inception_5a_pool_proj], axis=concat_axis, name='inception_5a/output')

#####
inception_5b_1x1 = Conv2D_bn(inception_5a_output, 384, (1,1), name='inception_5b/1x1')

inception_5b_3x3_reduce = Conv2D_bn(inception_5a_output, 192, (1,1), name='inception_5b/3x3_reduce')
inception_5b_3x3 = Conv2D_bn(inception_5b_3x3_reduce, 384, (3,3), name='inception_5b/3x3')

inception_5b_5x5_reduce = Conv2D_bn(inception_5a_output, 48, (1,1), name='inception_5b/5x5_reduce')
inception_5b_double3x3a = Conv2D_bn(inception_5b_5x5_reduce, 48, (3,3), name='inception_5b/double3x3a')
inception_5b_double3x3b = Conv2D_bn(inception_5b_double3x3a, 128, (3,3), name='inception_5b/double3x3b')

inception_5b_pool = AveragePooling2D(pool_size=(3,3), strides=(1,1), padding='same', name='inception_5b/pool')(inception_5a_output)
inception_5b_pool_proj = Conv2D_bn(inception_5b_pool, 128, (1,1), name='inception_5b/pool_proj')

inception_5b_output = concatenate([inception_5b_1x1, inception_5b_3x3, inception_5b_double3x3b, inception_5b_pool_proj], axis=concat_axis, name='inception_5b/output')

#####
inception_5c_1x1 = Conv2D_bn(inception_5b_output, 384, (1,1), name='inception_5c/1x1')

inception_5c_3x3_reduce = Conv2D_bn(inception_5b_output, 192, (1,1), name='inception_5c/3x3_reduce')
inception_5c_3x3 = Conv2D_bn(inception_5c_3x3_reduce, 384, (3,3), name='inception_5c/3x3')

inception_5c_5x5_reduce = Conv2D_bn(inception_5b_output, 48, (1,1), name='inception_5c/5x5_reduce')
inception_5c_double3x3a = Conv2D_bn(inception_5c_5x5_reduce, 48, (3,3), name='inception_5c/double3x3a')
inception_5c_double3x3b = Conv2D_bn(inception_5c_double3x3a, 128, (3,3), name='inception_5c/double3x3b')

inception_5c_pool = AveragePooling2D(pool_size=(3,3), strides=(1,1), padding='same', name='inception_5c/pool')(inception_5b_output)
inception_5c_pool_proj = Conv2D_bn(inception_5c_pool, 128, (1,1), name='inception_5c/pool_proj')

inception_5c_output = concatenate([inception_5c_1x1, inception_5c_3x3, inception_5c_double3x3b, inception_5c_pool_proj], axis=concat_axis, name='inception_5c/output')

#####
inception_5d_1x1 = Conv2D_bn(inception_5c_output, 384, (1,1), name='inception_5d/1x1')

inception_5d_3x3_reduce = Conv2D_bn(inception_5c_output, 192, (1,1), name='inception_5d/3x3_reduce')
inception_5d_3x3 = Conv2D_bn(inception_5d_3x3_reduce, 384, (3,3), name='inception_5d/3x3')

inception_5d_5x5_reduce = Conv2D_bn(inception_5c_output, 48, (1,1), name='inception_5d/5x5_reduce')
inception_5d_double3x3a = Conv2D_bn(inception_5d_5x5_reduce, 48, (3,3), name='inception_5d/double3x3a')
inception_5d_double3x3b = Conv2D_bn(inception_5d_double3x3a, 128, (3,3), name='inception_5d/double3x3b')

inception_5d_pool = AveragePooling2D(pool_size=(3,3), strides=(1,1), padding='same', name='inception_5d/pool')(inception_5c_output)
inception_5d_pool_proj = Conv2D_bn(inception_5d_pool, 128, (1,1), name='inception_5d/pool_proj')

inception_5d_output = concatenate([inception_5d_1x1, inception_5d_3x3, inception_5d_double3x3b, inception_5d_pool_proj], axis=concat_axis, name='inception_5d/output')

#####
inception_5e_1x1 = Conv2D_bn(inception_5d_output, 384, (1,1), name='inception_5e/1x1')

inception_5e_3x3_reduce = Conv2D_bn(inception_5d_output, 192, (1,1), name='inception_5e/3x3_reduce')
inception_5e_3x3 = Conv2D_bn(inception_5e_3x3_reduce, 384, (3,3), name='inception_5e/3x3')

inception_5e_5x5_reduce = Conv2D_bn(inception_5d_output, 48, (1,1), name='inception_5e/5x5_reduce')
inception_5e_double3x3a = Conv2D_bn(inception_5e_5x5_reduce, 48, (3,3), name='inception_5e/double3x3a')
inception_5e_double3x3b = Conv2D_bn(inception_5e_double3x3a, 128, (3,3), name='inception_5e/double3x3b')

inception_5e_pool = AveragePooling2D(pool_size=(3,3), strides=(1,1), padding='same', name='inception_5e/pool')(inception_5d_output)
```

```

inception_5e_pool_proj = Conv2D_bn(inception_5e_pool,128,(1,1),name='inception_5e/pool_proj')
inception_5e_output = concatenate([inception_5e_lx1,inception_5e_3x3,inception_5e_double3x3b,inception_5e_pool_proj],axis=concat_axis,name='inception_5e/output')
#####
inception_5f_lx1 = Conv2D_bn(inception_5e_output,384,(1,1),name='inception_5f/lx1')
inception_5f_3x3_reduce = Conv2D_bn(inception_5e_output,192,(1,1),name='inception_5f/3x3_reduce')
inception_5f_3x3 = Conv2D_bn(inception_5f_3x3_reduce,384,(3,3),name='inception_5f/3x3')
inception_5f_5x5_reduce = Conv2D_bn(inception_5e_output,48,(1,1),name='inception_5f/5x5_reduce')
inception_5f_double3x3a = Conv2D_bn(inception_5f_5x5_reduce,48,(3,3),name='inception_5f/double3x3a')
inception_5f_double3x3b = Conv2D_bn(inception_5f_double3x3a,128,(3,3),name='inception_5f/double3x3b')
inception_5f_pool = AveragePooling2D(pool_size=(3,3),strides=(1,1),padding='same',name='inception_5f/pool')(inception_5e_output)
inception_5f_pool_proj = Conv2D_bn(inception_5f_pool,128,(1,1),name='inception_5f/pool_proj')
inception_5f_output = concatenate([inception_5f_lx1,inception_5f_3x3,inception_5f_double3x3b,inception_5f_pool_proj],axis=concat_axis,name='inception_5f/output')
#####
inception_5g_lx1 = Conv2D_bn(inception_5f_output,384,(1,1),name='inception_5g/lx1')
inception_5g_3x3_reduce = Conv2D_bn(inception_5f_output,192,(1,1),name='inception_5g/3x3_reduce')
inception_5g_3x3 = Conv2D_bn(inception_5g_3x3_reduce,384,(3,3),name='inception_5g/3x3')
inception_5g_5x5_reduce = Conv2D_bn(inception_5f_output,48,(1,1),name='inception_5g/5x5_reduce')
inception_5g_double3x3a = Conv2D_bn(inception_5g_5x5_reduce,48,(3,3),name='inception_5g/double3x3a')
inception_5g_double3x3b = Conv2D_bn(inception_5g_double3x3a,128,(3,3),name='inception_5g/double3x3b')
inception_5g_pool = AveragePooling2D(pool_size=(3,3),strides=(1,1),padding='same',name='inception_5g/pool')(inception_5f_output)
inception_5g_pool_proj = Conv2D_bn(inception_5g_pool,128,(1,1),name='inception_5g/pool_proj')
inception_5g_output = concatenate([inception_5g_lx1,inception_5g_3x3,inception_5g_double3x3b,inception_5g_pool_proj],axis=concat_axis,name='inception_5g/output')
#####
inception_5h_lx1 = Conv2D_bn(inception_5g_output,384,(1,1),name='inception_5h/lx1')
inception_5h_3x3_reduce = Conv2D_bn(inception_5g_output,192,(1,1),name='inception_5h/3x3_reduce')
inception_5h_3x3 = Conv2D_bn(inception_5h_3x3_reduce,384,(3,3),name='inception_5h/3x3')
inception_5h_5x5_reduce = Conv2D_bn(inception_5g_output,48,(1,1),name='inception_5h/5x5_reduce')
inception_5h_double3x3a = Conv2D_bn(inception_5h_5x5_reduce,48,(3,3),name='inception_5h/double3x3a')
inception_5h_double3x3b = Conv2D_bn(inception_5h_double3x3a,128,(3,3),name='inception_5h/double3x3b')
inception_5h_pool = AveragePooling2D(pool_size=(3,3),strides=(1,1),padding='same',name='inception_5h/pool')(inception_5g_output)
inception_5h_pool_proj = Conv2D_bn(inception_5h_pool,128,(1,1),name='inception_5h/pool_proj')
inception_5h_output = concatenate([inception_5h_lx1,inception_5h_3x3,inception_5h_double3x3b,inception_5h_pool_proj],axis=concat_axis,name='inception_5h/output')
#####
inception_5i_lx1 = Conv2D_bn(inception_5h_output,384,(1,1),name='inception_5i/lx1')
inception_5i_3x3_reduce = Conv2D_bn(inception_5h_output,192,(1,1),name='inception_5i/3x3_reduce')
inception_5i_3x3 = Conv2D_bn(inception_5i_3x3_reduce,384,(3,3),name='inception_5i/3x3')
inception_5i_5x5_reduce = Conv2D_bn(inception_5h_output,48,(1,1),name='inception_5i/5x5_reduce')
inception_5i_double3x3a = Conv2D_bn(inception_5i_5x5_reduce,48,(3,3),name='inception_5i/double3x3a')
inception_5i_double3x3b = Conv2D_bn(inception_5i_double3x3a,128,(3,3),name='inception_5i/double3x3b')
inception_5i_pool = AveragePooling2D(pool_size=(3,3),strides=(1,1),padding='same',name='inception_5i/pool')(inception_5h_output)
inception_5i_pool_proj = Conv2D_bn(inception_5i_pool,128,(1,1),name='inception_5i/pool_proj')
inception_5i_output = concatenate([inception_5i_lx1,inception_5i_3x3,inception_5i_double3x3b,inception_5i_pool_proj],axis=concat_axis,name='inception_5i/output')
#####
inception_5j_lx1 = Conv2D_bn(inception_5i_output,384,(1,1),name='inception_5j/lx1')
inception_5j_3x3_reduce = Conv2D_bn(inception_5i_output,192,(1,1),name='inception_5j/3x3_reduce')
inception_5j_3x3 = Conv2D_bn(inception_5j_3x3_reduce,384,(3,3),name='inception_5j/3x3')
inception_5j_5x5_reduce = Conv2D_bn(inception_5i_output,48,(1,1),name='inception_5j/5x5_reduce')
inception_5j_double3x3a = Conv2D_bn(inception_5j_5x5_reduce,48,(3,3),name='inception_5j/double3x3a')
inception_5j_double3x3b = Conv2D_bn(inception_5j_double3x3a,128,(3,3),name='inception_5j/double3x3b')
inception_5j_pool = AveragePooling2D(pool_size=(3,3),strides=(1,1),padding='same',name='inception_5j/pool')(inception_5i_output)
inception_5j_pool_proj = Conv2D_bn(inception_5j_pool,128,(1,1),name='inception_5j/pool_proj')
inception_5j_output = concatenate([inception_5j_lx1,inception_5j_3x3,inception_5j_double3x3b,inception_5j_pool_proj],axis=concat_axis,name='inception_5j/output')
#####
# Pooling
#####
pool5_7x7_s1 = AveragePooling2D(pool_size=(7,7),strides=(1,1),name='pool5/7x7_s2')(inception_5j_output)
loss3_flat = Flatten()(pool5_7x7_s1)
loss3_classifier = Dense(1000,name='loss3/classifier',kernel_regularizer=L2(L2_WEIGHT_DECAY))(loss3_flat)
loss3_classifier_act = Activation('softmax',name='prob')(loss3_classifier)
deepinception = Model(inputs=img_input, outputs=[loss1_classifier_act, loss2_classifier_act, loss3_classifier_act])#, loss3_flat
if weights_path:
    deepinception.load_weights(weights_path)
return deepinception

```